

Summer 6-19-2013

An Overview of the Materials Physics Group And Potential Collaborations with LAPLACE

JR Dennison
Utah State University

Follow this and additional works at: https://digitalcommons.usu.edu/mp_presentations



Part of the [Physics Commons](#)

Recommended Citation

Dennison, JR, "An Overview of the Materials Physics Group And Potential Collaborations with LAPLACE" (2013). Invited Seminar, Laplace Laboratoire Plasma et Conversion D'Energie, Universite Paul Sabatier, Toulouse, France. *Presentations*. Paper 29.

https://digitalcommons.usu.edu/mp_presentations/29

This Presentation is brought to you for free and open access by the Materials Physics at DigitalCommons@USU. It has been accepted for inclusion in Presentations by an authorized administrator of DigitalCommons@USU. For more information, please contact digitalcommons@usu.edu.



Laboratory on Plasma & Conversion of Energy



Toulouse, France

19 June, 2013

An Overview of the Materials Physics Group And Potential Collaborations with LAPLACE

J.R. Dennison

Materials Physics Group

Physics Department, Utah State University

Logan, Utah USA



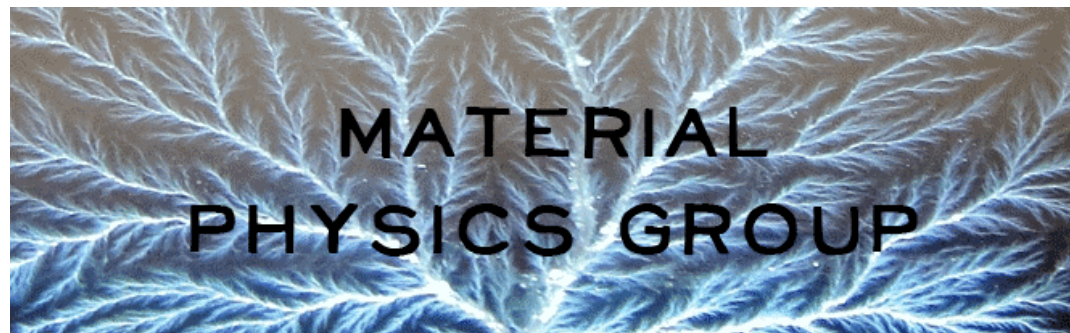


Utah State University



USU Materials Physics Group

Utah State University
Logan, Utah, USA



Acknowledgements

Support & Collaborations

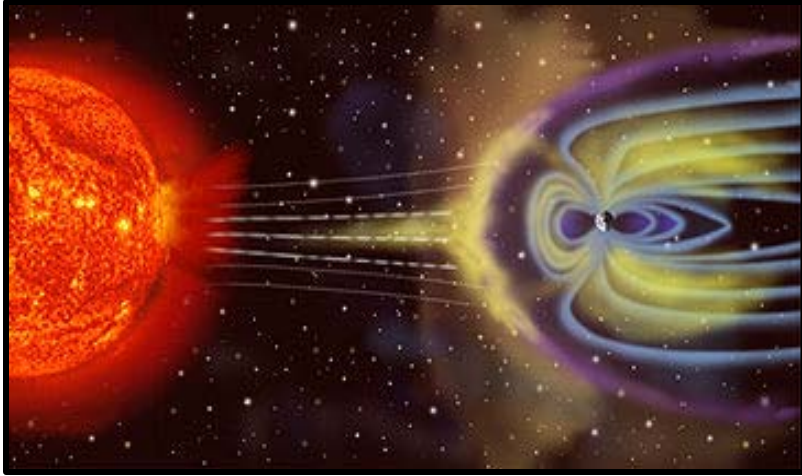
***NASA SEE Program
JWST (GSFC/MSFC)
SPM (JHU/APL)
RBSP (JHU/APL)
Solar Sails (JPL)
AFRL
Boeing
Ball Aerospace
Orbital***

***National Research
Council***

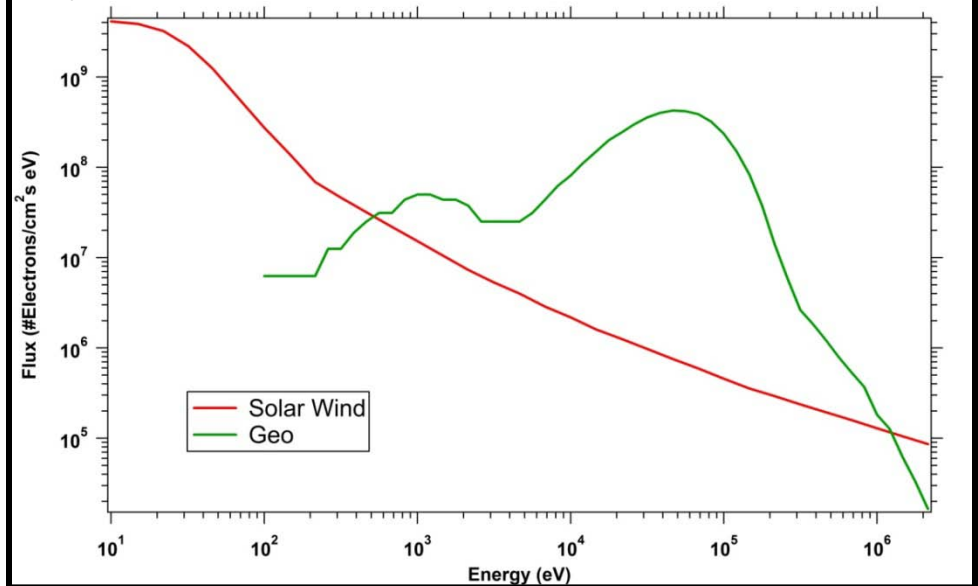


USU Materials Physics Group

Solar wind and Earth's magento-sphere structure.



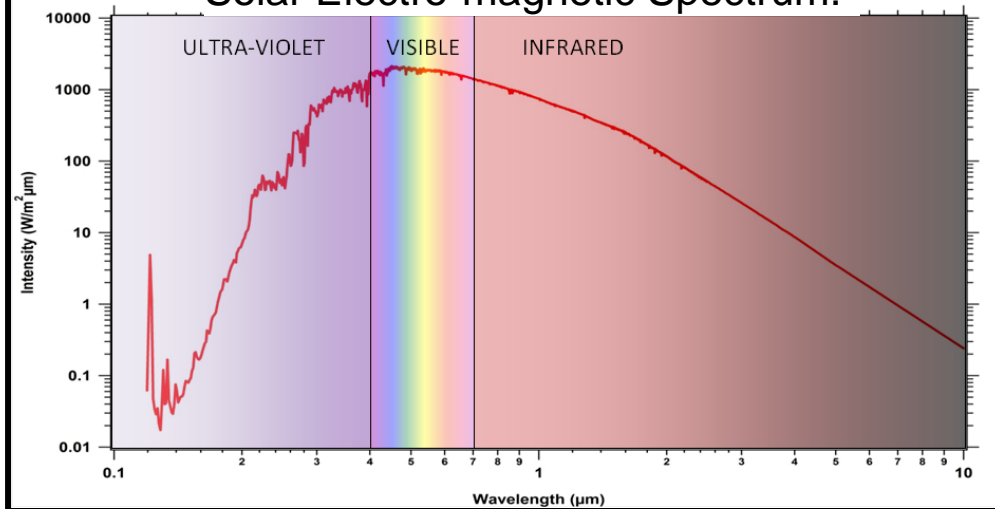
Typical Space Electron Flux Spectra [Larsen].



Incident Fluxes of:

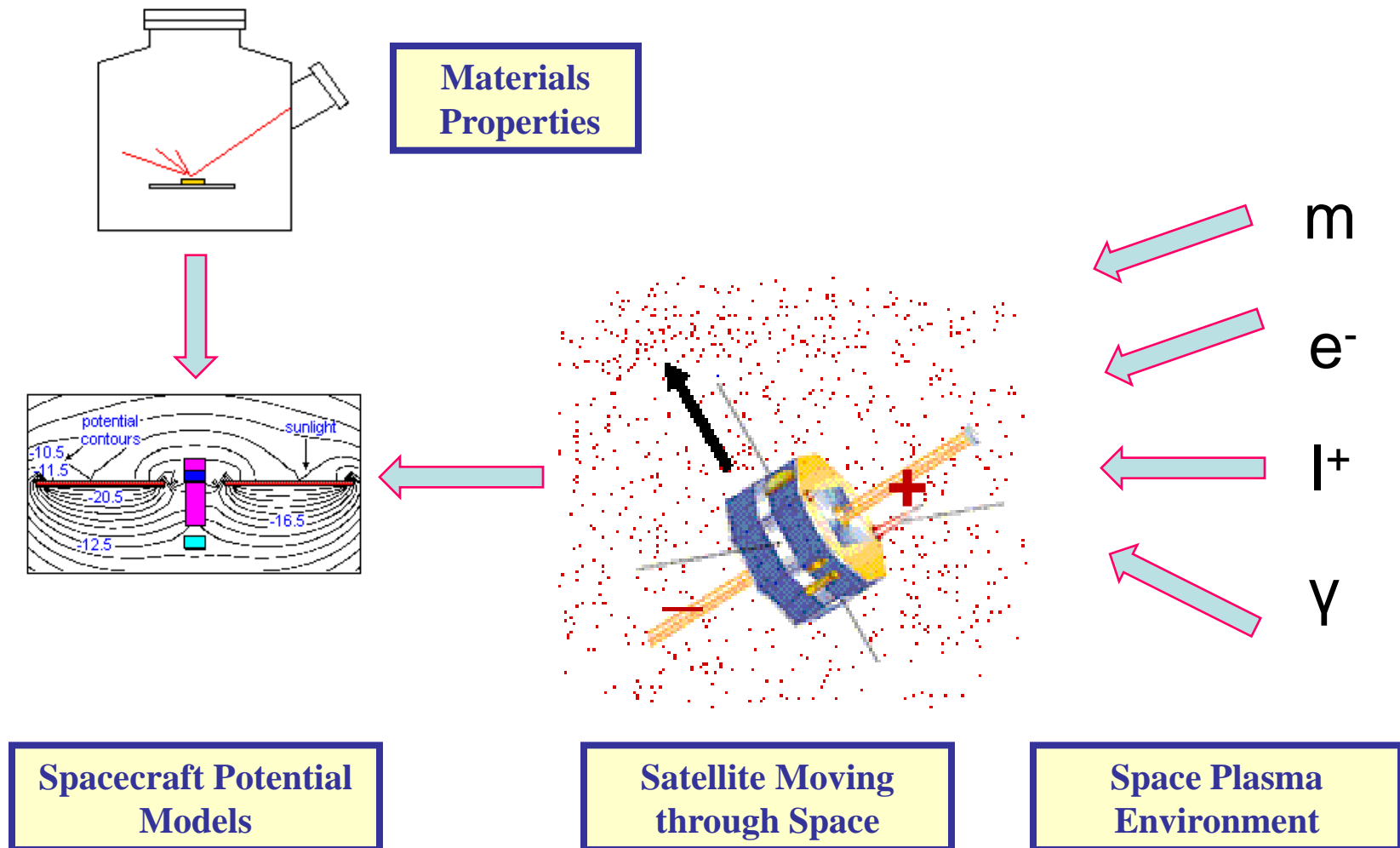
- **Electrons**
- **Ions**
- **Photons**
- **Particles**

Solar Electro-magnetic Spectrum.





A simplified approach to spacecraft charging modeling...



This results in a complex dynamic interplay between space environment, satellite motion, and materials properties



Specific focus of our work is the change in materials properties as a function of time , position, energy, and charge:

- **Time (Aging), t**
- **Position (z)**
 - Charge distributions, $Q(z,t)$
 - Surface voltage, $\Delta V(xy,t)$
- **Energy**
 - Temperature, $k_B T$
 - Deposited Energy (Dose), D
 - Power Deposition (Dose) Rate, \dot{D}
- **Charge**
 - Accumulated Charge, ΔQ or $\Delta V(Q, \Delta V, D, \dot{D}, t)$
 - Charge Profiles, $Q(z,t)$
 - Charge Rate (Current), \dot{Q}
 - Conductivity Profiles, $\sigma(z,t,Q,\dot{Q},D,\dot{D})$
 - Electron emission (e^- , I^+ , Γ)
- **Light emission**
 - Cathodoluminescence $I_{\Gamma}(t,xy,Q,D,\dot{D})$
 - Arcing $I_{\Gamma}(t,xy,Q,D,\dot{D})$, $\dot{Q}_{\Gamma}(t,z,Q,D,\dot{D})$

What do you need to know about the materials properties?

Charging codes such as NASCAP-2K or SPENVIS and NUMIT2 or DICTAT require:

Charge Accumulation

- **Electron yields**
- **Ion yields**
- **Photoyields**
- **Luminescence**

Charge Transport

- **Conductivity**
- **RIC**
- **Dielectric Constant**
- **ESD**
- **Range**

ABSOLUTE values as functions of materials species, flux, fluence, and energy.

Table 2.1. Parameters for NASCAP Materials Properties

Parameter	Value
[1] Relative dielectric constant; ϵ_r (Input as 1 for conductors)	1, NA
[2] Dielectric film thickness; d	0 m, NA
[3] Bulk conductivity; σ_o (Input as -1 for conductors)	-1; $(4.26 \pm 0.04) \cdot 10^7 \text{ ohm}^{-1} \cdot \text{m}^{-1}$
[4] Effective mean atomic number $\langle Z_{\text{eff}} \rangle$	50.9 ± 0.5
[5] Maximum SE yield for electron impact; δ_{max}	1.47 ± 0.01
[6] Primary electron energy for δ_{max} ; E_{max}	$(0.569 \pm 0.07) \text{ keV}$
[7] First coefficient for bi-exponential range law, b_1	1 Å, NA
[8] First power for bi-exponential range law, n_1	1.39 ± 0.02
[9] Second coefficient for bi-exponential range law, b_2	0 Å
[10] Second power for bi-exponential range law, n_2	0
[11] SE yield due to proton impact $\delta^H(1\text{keV})$	0.3364 ± 0.0003
[12] Incident proton energy for δ^H_{max} ; E^H_{max}	$(1238 \pm 30) \text{ keV}$
[13] Photoelectron yield, normally incident sunlight, j_{pho}	$(3.64 \pm 0.4) \cdot 10^{-5} \text{ A} \cdot \text{m}^{-2}$
[14] Surface resistivity; ρ_s (Input as -1 for non-conductors)	-1 ohms \cdot square $^{-1}$, NA
[15] Maximum potential before discharge to space; V_{max}	10000 V, NA
[16] Maximum surface potential difference before dielectric breakdown discharge; V_{punch}	2000 V, NA
[17] Coefficient of radiation-induced conductivity, σ_r ; k	0 ohms $^{-1} \cdot \text{m}^{-1}$, NA
[18] Power of radiation-induced conductivity, σ_r ; Δ	0, NA

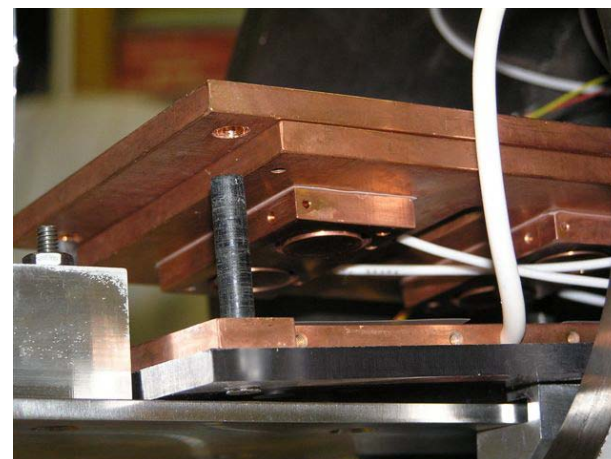
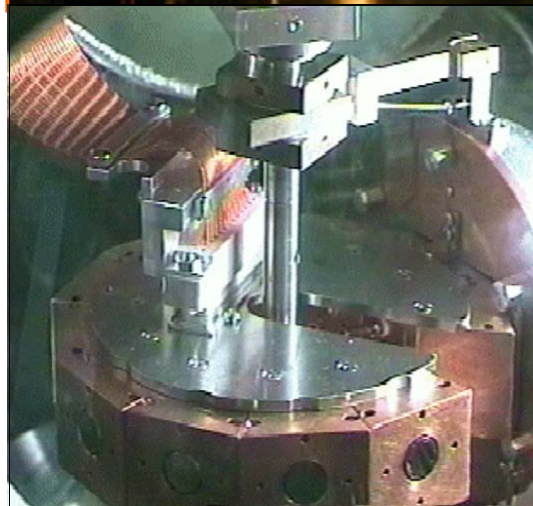
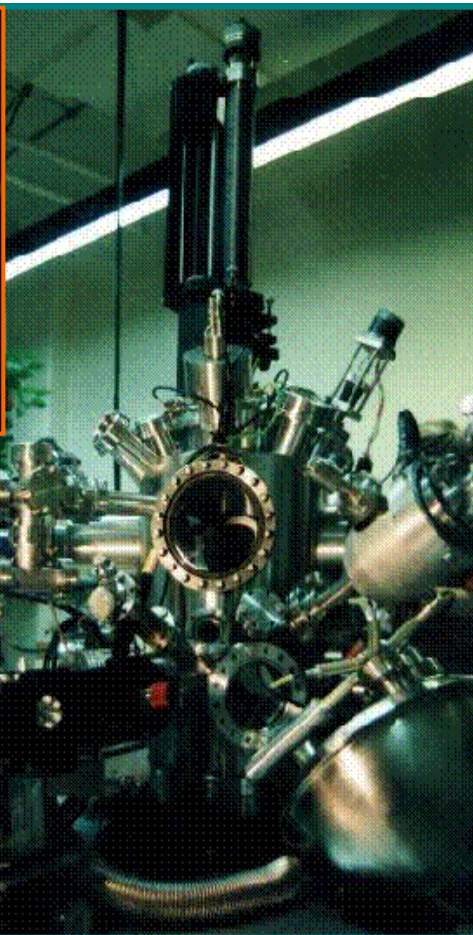
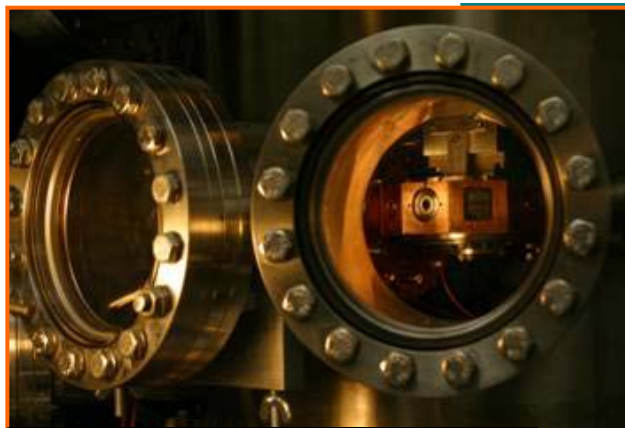
Materials Physics Group Measurement Capabilities

Electron Emission
Ion Yield

Photoyield
Luminescence

Conductivity
Electrostatic Discharge

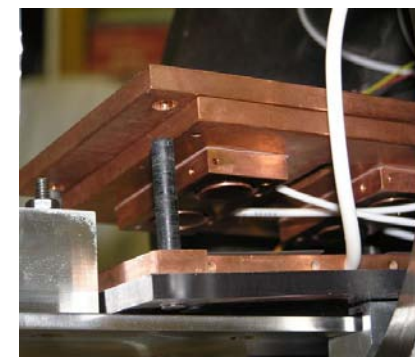
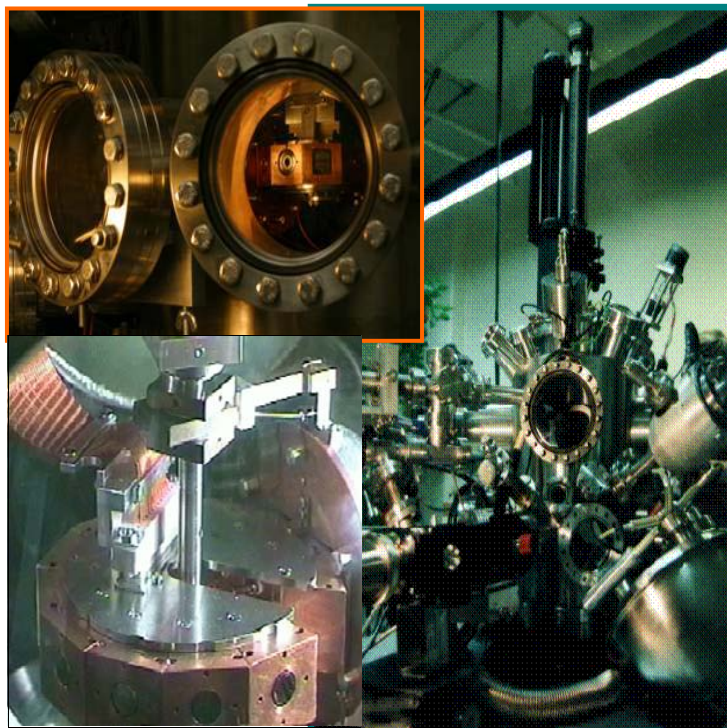
Radiation Induced Cond.
Radiation Damage



Dependence on: Press., Temp., Charge, E-field, Dose, Dose Rate

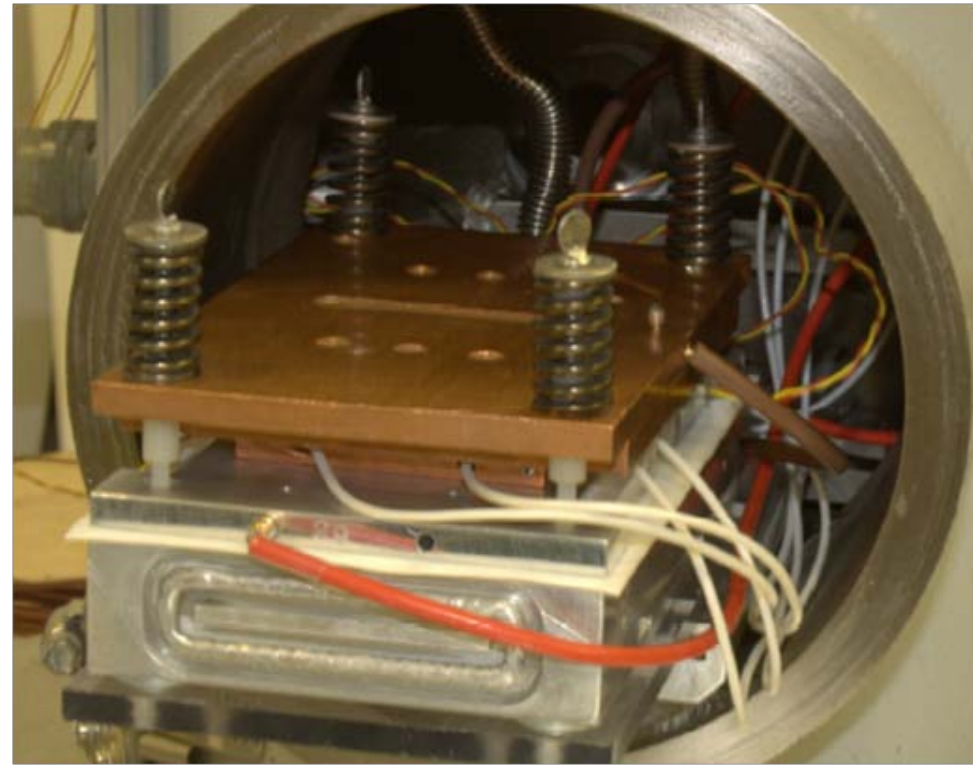
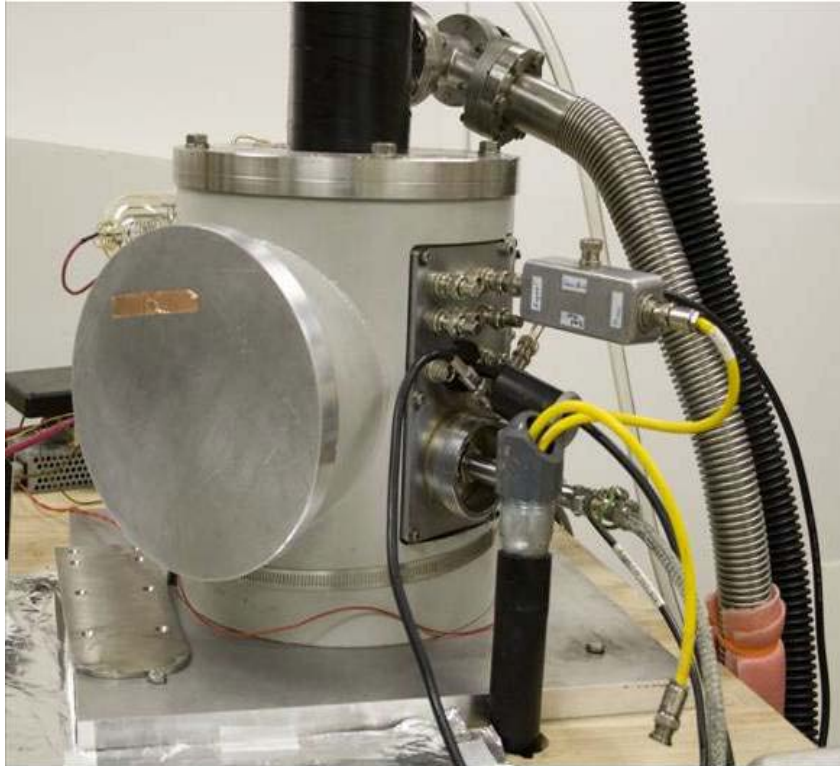
Absolute Yields

- SEE, BSE, emission spectra , (<20 eV to 30 keV)
- Angle resolved electron emission spectra
- Photoyield (~160 nm to 1200 nm)
- Ion yield (He, Ne, Ar, Kr, Xe; <100 eV to 5 keV)
- Cathodoluminescence (200 nm to 5000 nm)
- No-charge “Intrinsic” Yields
- T (<40 K to >400 K)



- Conductivity ($<10^{-22}$ [ohm-cm] $^{-1}$)
- Surface Charge (<1 V to >15 kV)
- ESD (low T, long duration)
- Radiation Induced Conductivity (RIC)
- Evolution of internal charge distributions (EA)
- Multilayers, contamination, surface modification
- Radiation damage
- Modeling
- Sample Characterization

Extremely Low Conductivity



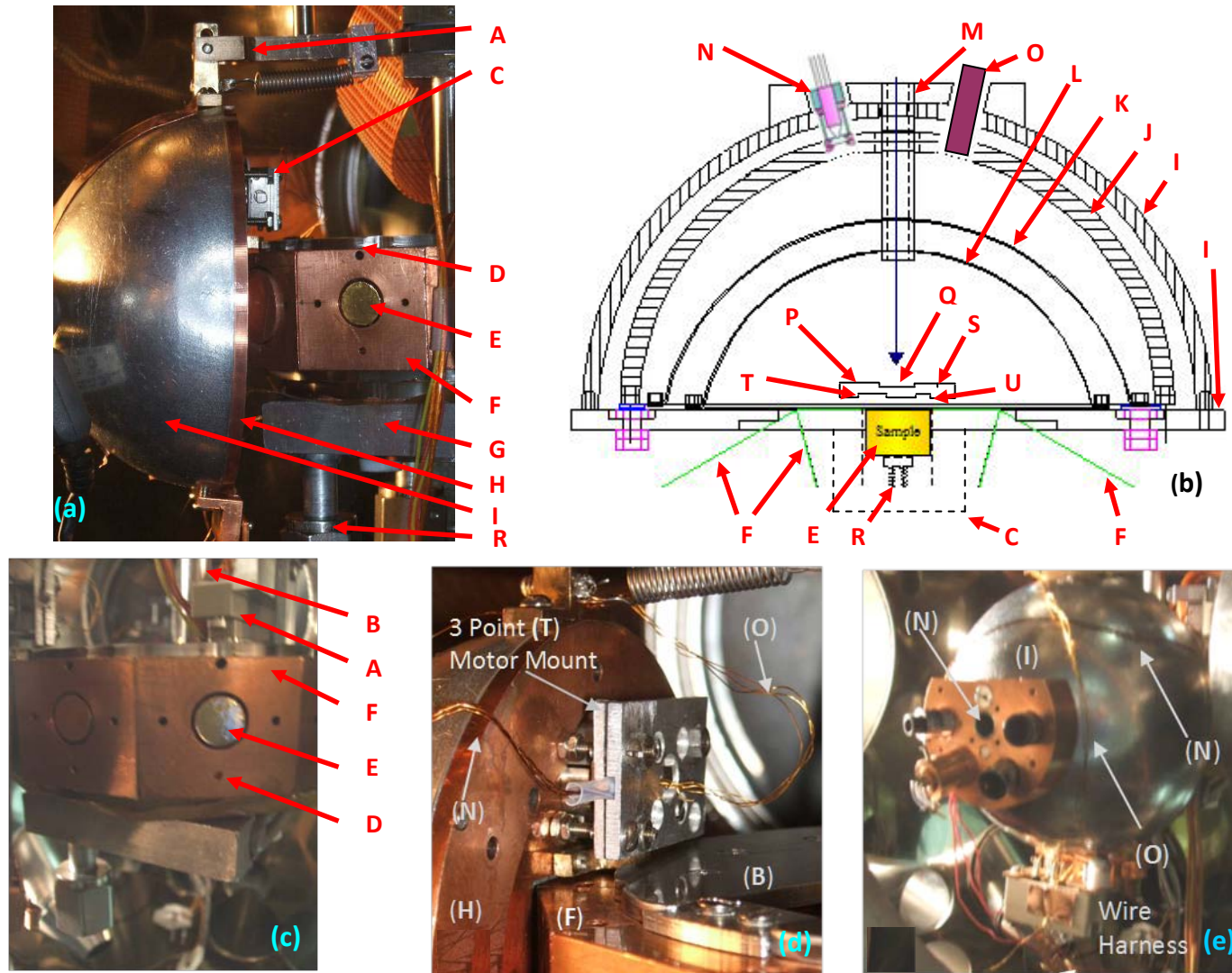
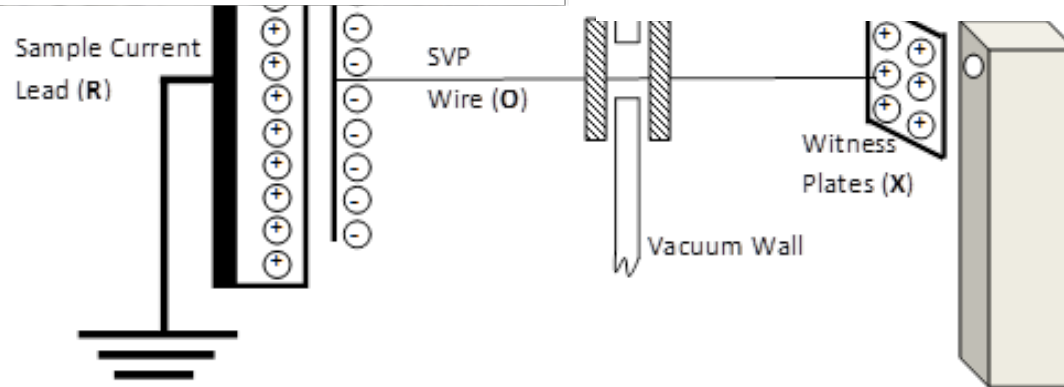
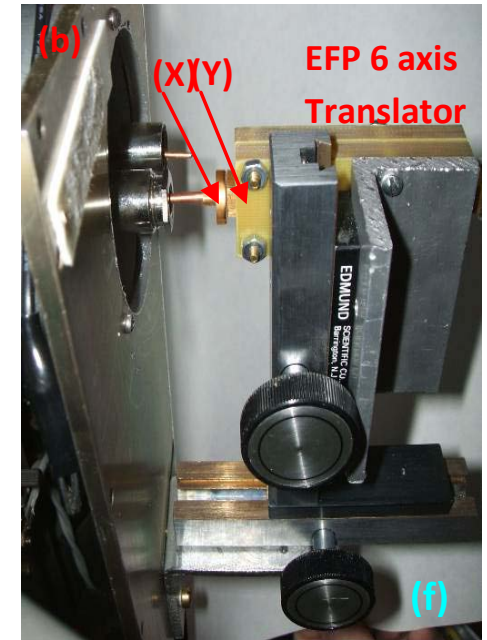
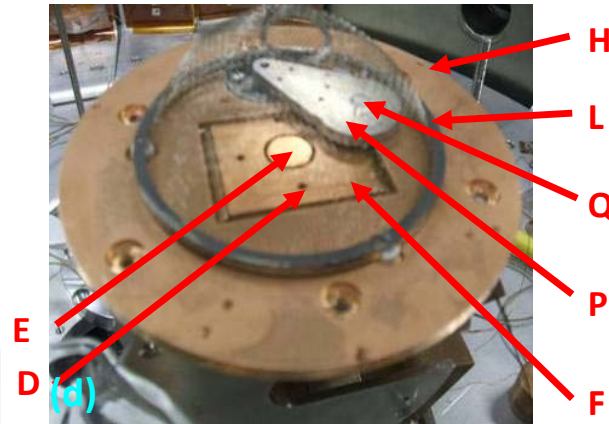
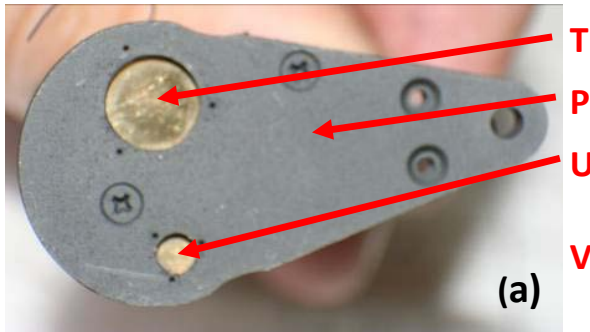


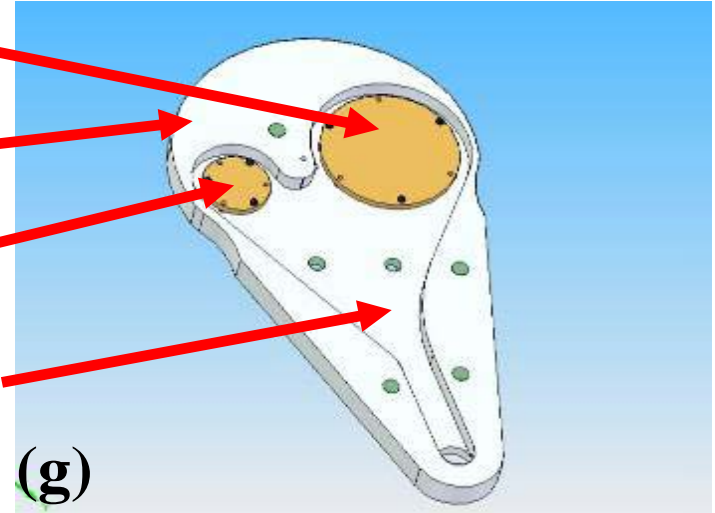
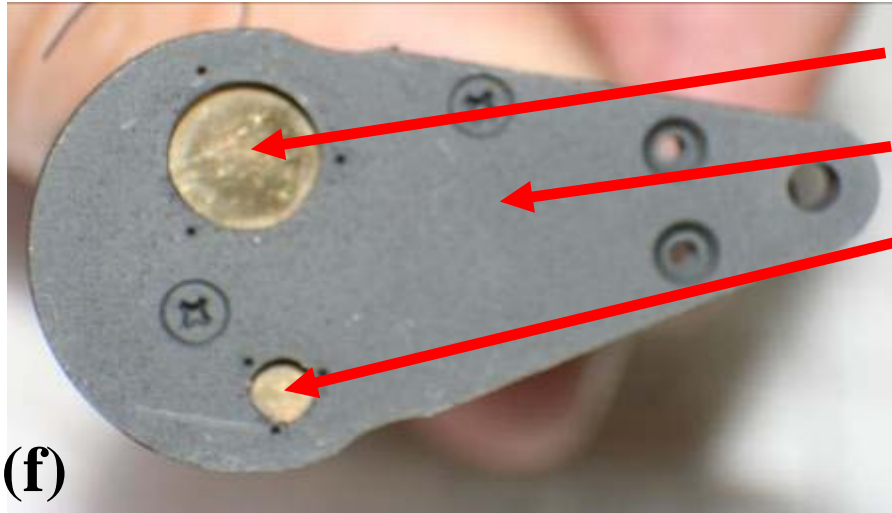
Fig. 2. Hemispherical Grid Retarding Field Analyzer (HGRFA). (a) Photograph of sample stage and HGRFA detector (side view). (b) Cross section of HGRFA. (c) Photograph of sample stage showing sample and cooling reservoir. (d) Side view of the mounting of the stepper motor. (e) Isometric view of the HGRFA detailing the flood gun, optical ports, and wire harness.

Surface Voltage



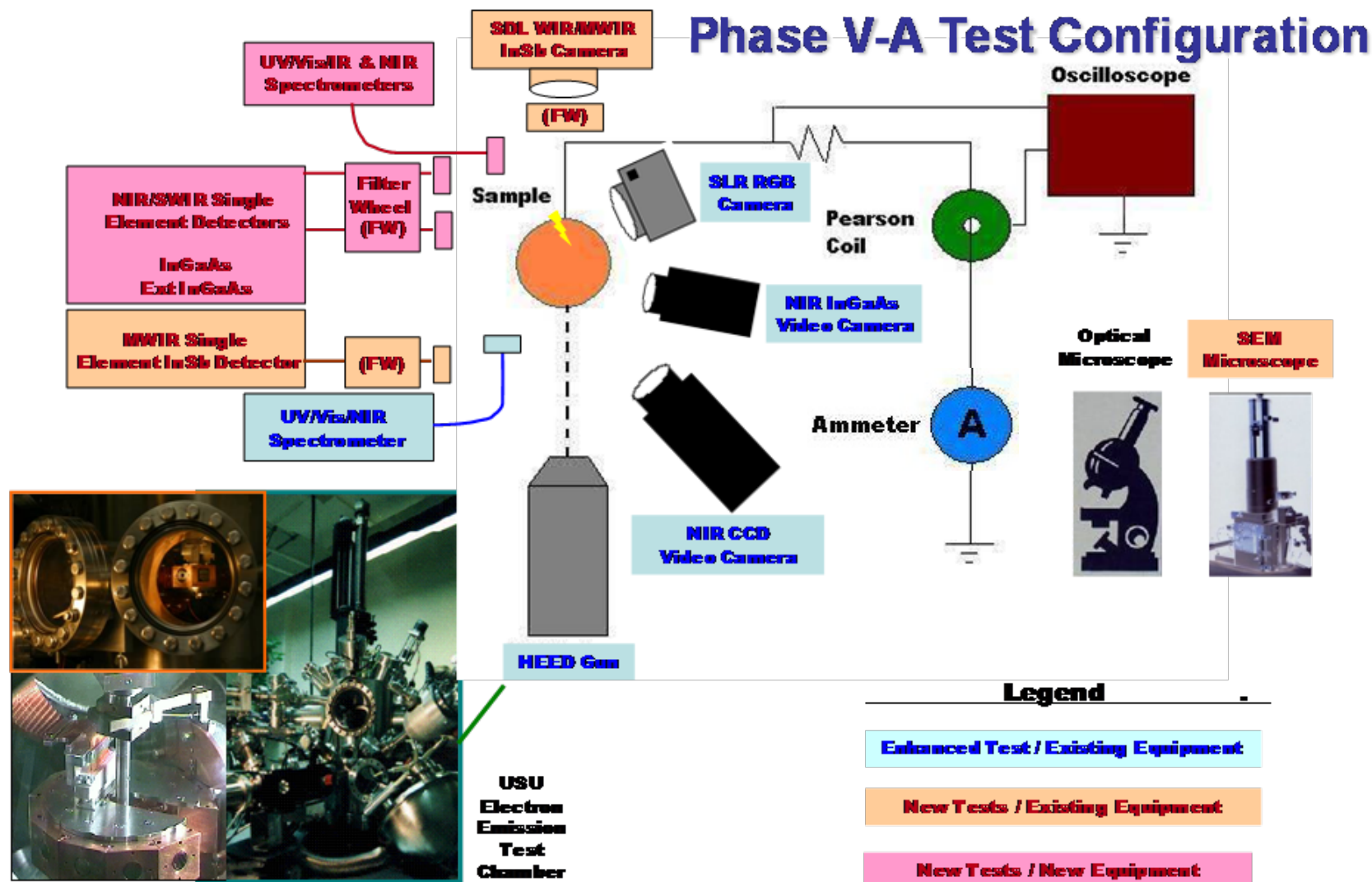


SVP (Surface Voltage Probe)



- | | | |
|--|--------------------------------------|----------------------------------|
| A HGRFA Hinged Mount | I HGRFA Hemispherical Shield | R Sample Current Lead |
| B Sample Carousel/HGRFA Rotation Shaft | J HGRFA Collector | S SVP Faraday Cup |
| C UHV Stepper Motor | K HGRFA Bias Grid | T SVP 7 mm Diameter Au Electrode |
| D Sample Block Faraday Cup | L HGRFA Inner Grid | U SVP 3 mm Diameter Au Electrode |
| E Sample (10 mm) | M HGRFA Drift Tube | V SVP Wiring Channel |
| F Sample Block | N Electron Flood Gun | W EFTP Vacuum Feedthrough |
| G Cryogen Reservoir | O LED Light Source | X EFTP Witness Plate |
| H HGRFA Face Plate | P Surface Voltage Probe (SVP) | Y Electrostatic Field Probe |
| | Q Au disc Electron Emission Standard | Z Probe XYZ Translator |

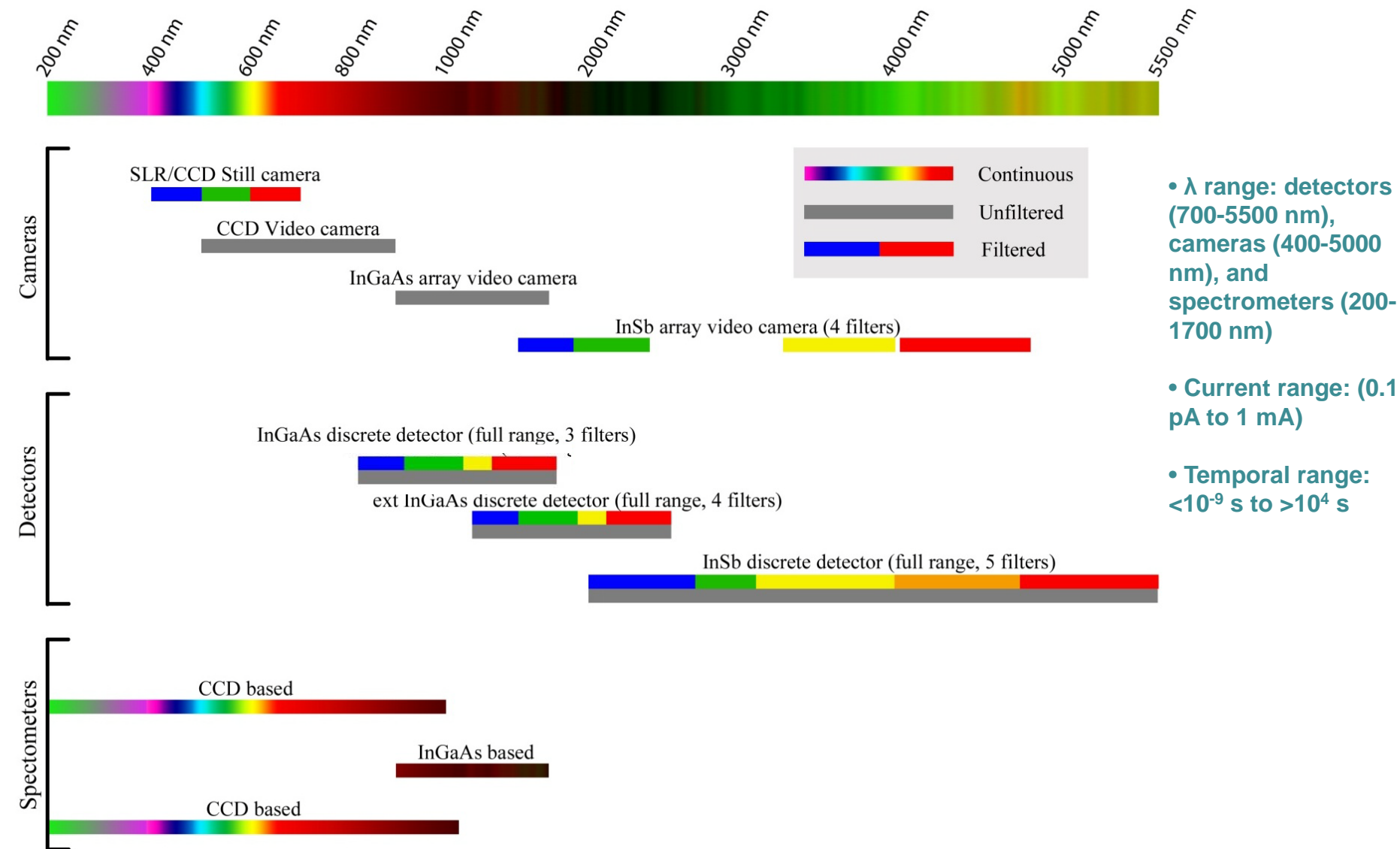
Luminescence/Arc/Flare Test Configuration



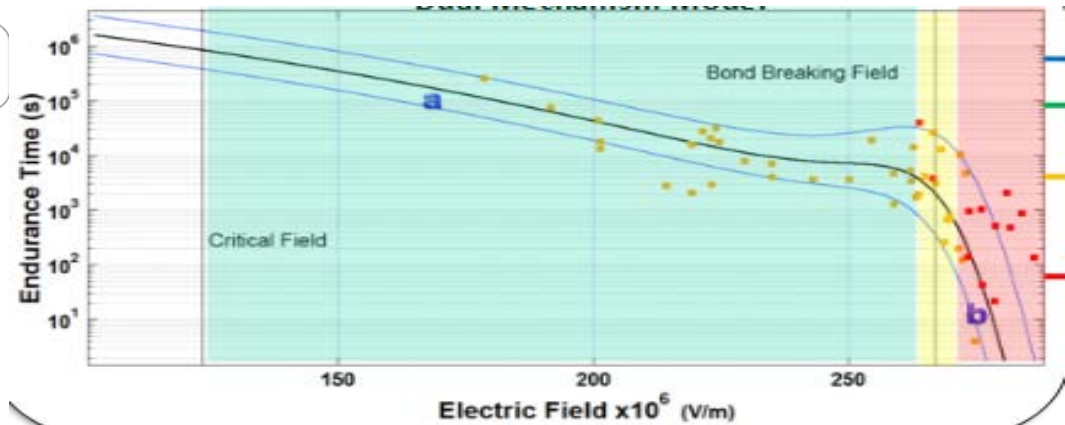
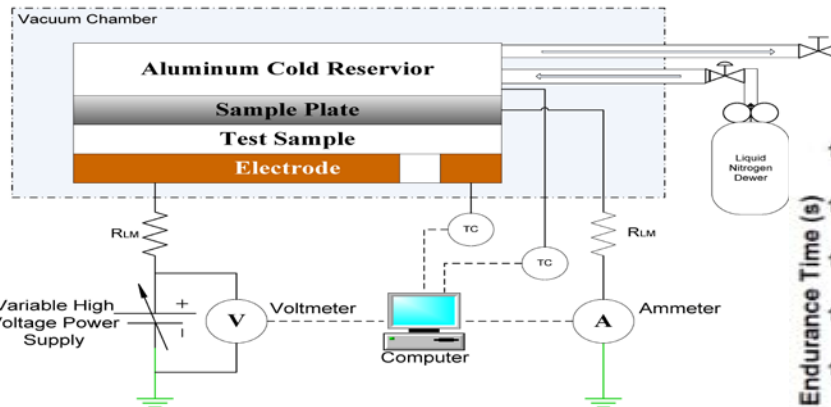
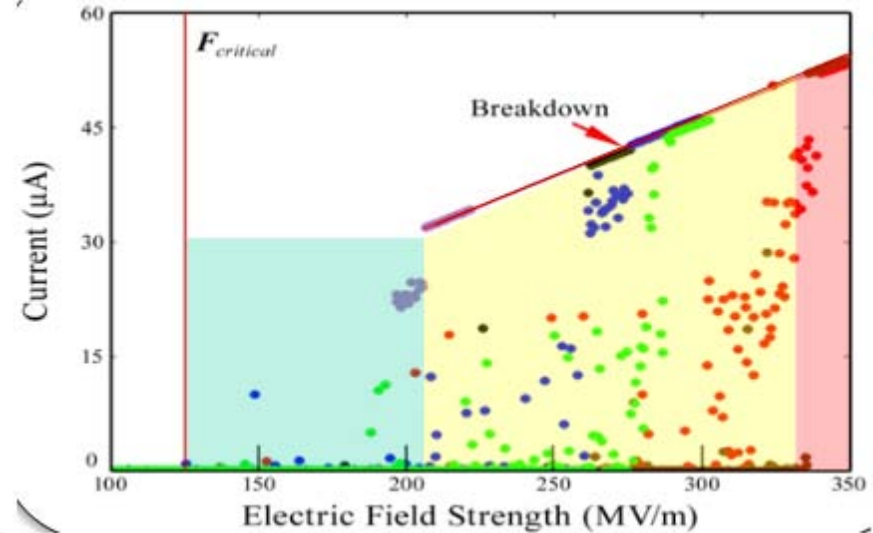
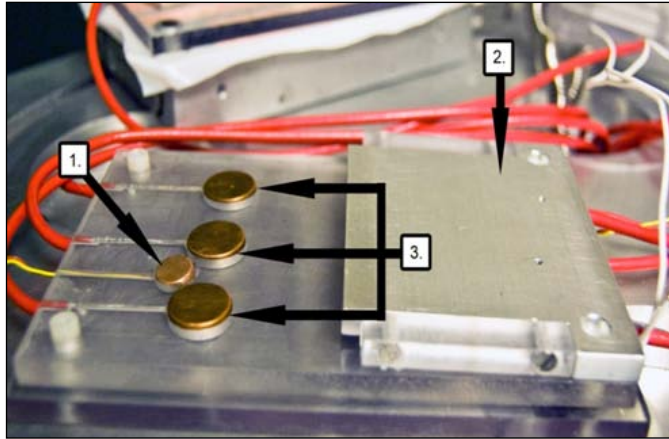
Sample cooled with I-N₂ to 100-135 K.
Chamber walls at ambient.



Luminescence/Arc/Flare Test Configuration



Electrostatic Breakdown



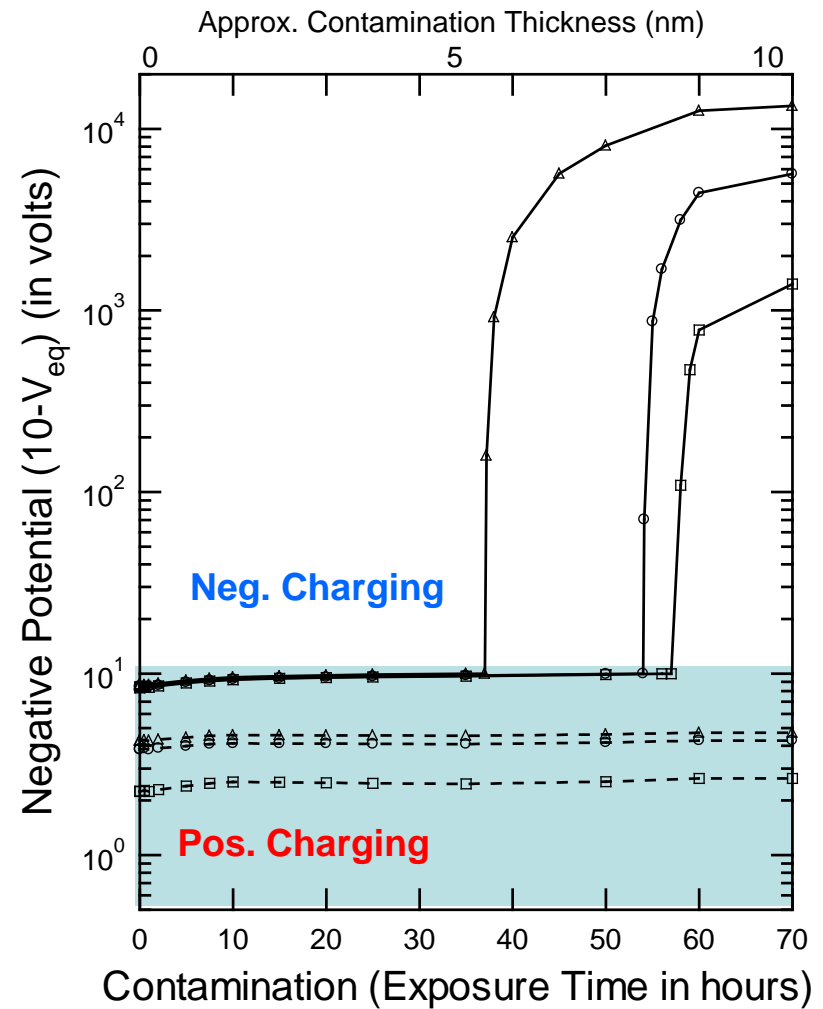
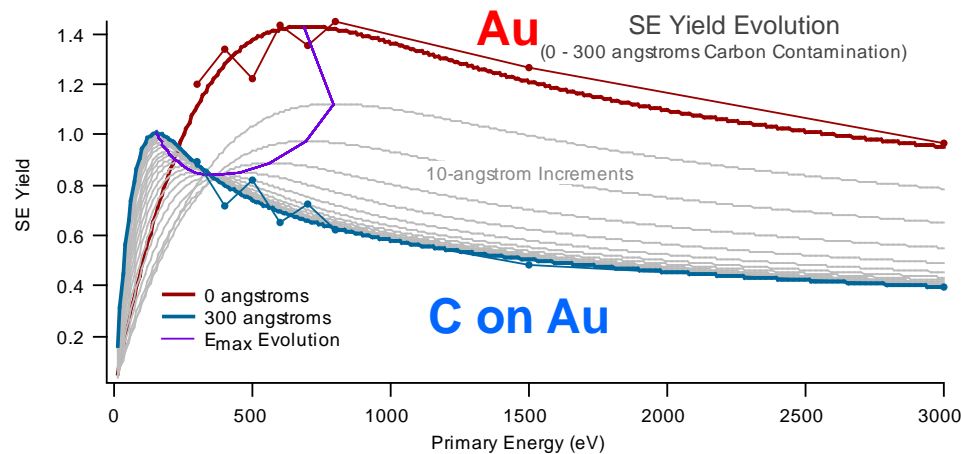


Recent and Current Projects

Case I: Evolution of Contamination and Oxidation

“All spacecraft surfaces are eventually carbon...”
--C. Purvis

This led to lab studies by Davies, Kite, and Chang



Case I: Evolution of Contamination and Oxidation

Wake Side

- 13 Grounded Samples
- 12 Biased Samples: for 3 sets of 4 samples with low current biases for charge-enhanced contamination studies.

- 6 Concealed Samples

Sample Holders

- Holder area 5 cm x 15 cm
- 9 mm diameter exposed sample area

Grounded Guard Plate

-5 VDC

+5 VDC

-15 VDC

Before

After

SUSpECs on MISSE-6

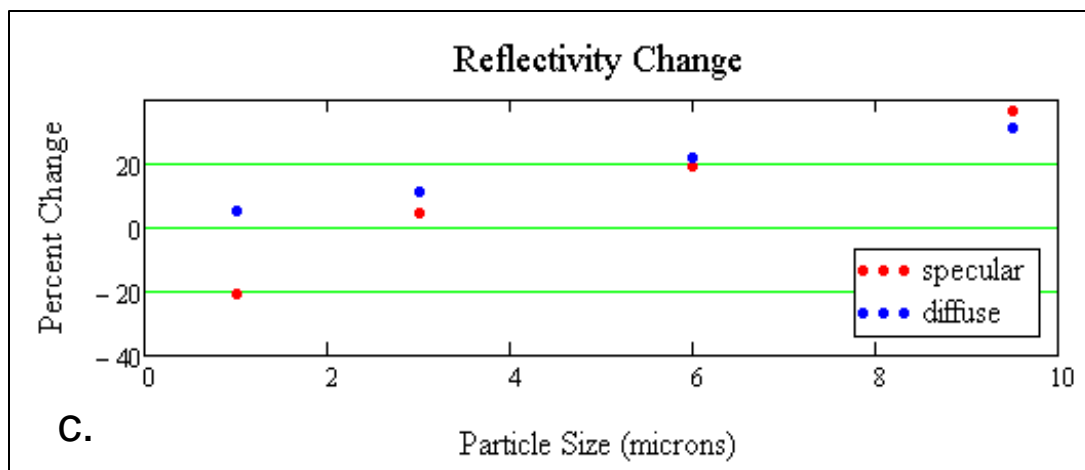
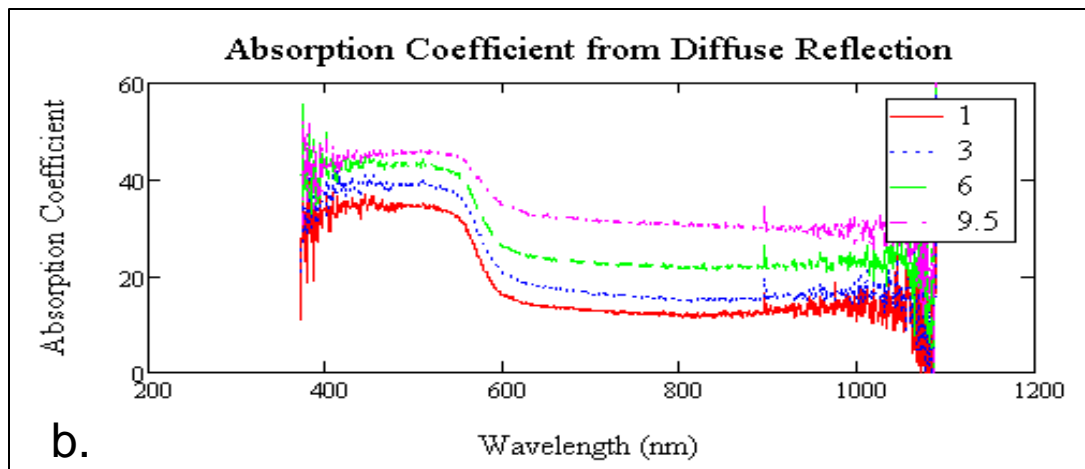
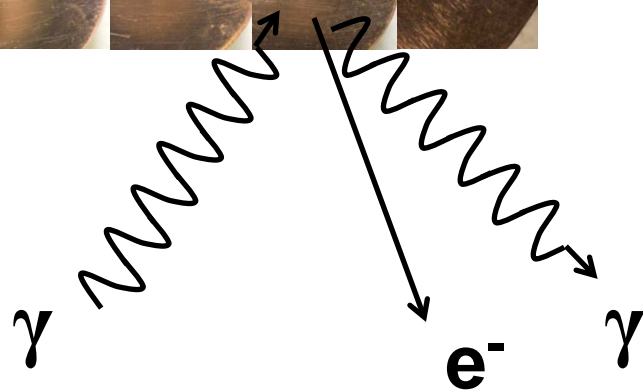
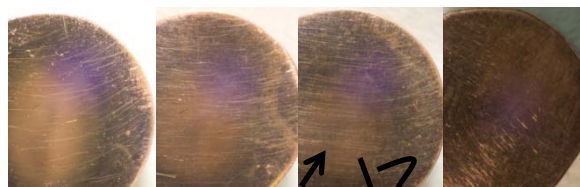
Ag coated Mylar with micrometeoroid impact

See poster by Dennison,
Evans and Prebola

Case II: Surface Modification

Diffuse and Specular Reflectivity changes with surface roughness

Successive stages of roughened Cu



View photon (electron) scattering as a competition for deposited energy and charge:

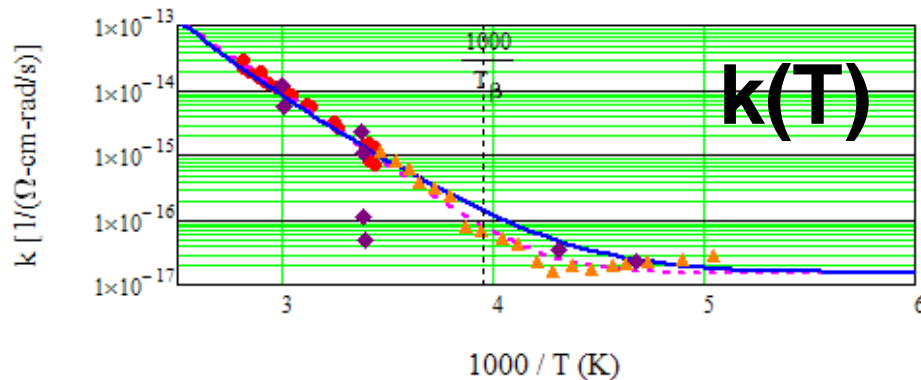
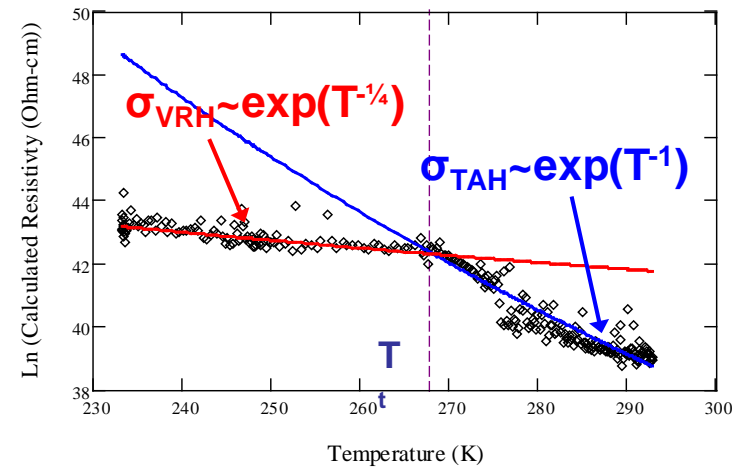
- Reflectivity— γ out (Luminescence— γ out)
- Photoyield— e^- out (SE/BSE— e^- out)

Case III: Temperature Effects

Strong T Dependence for Insulators

Charge Transport

- Conductivity
- RIC
- Dielectric Constant
- ESD



- Yagahi, 1963 Data
- - - Exponential Fit
- Power Law Fit
- ▲▲▲ Fowler, 1956 Data
- ◆◆ USU Data

Uniform Trap Density

$$\Delta(T) \rightarrow 1$$

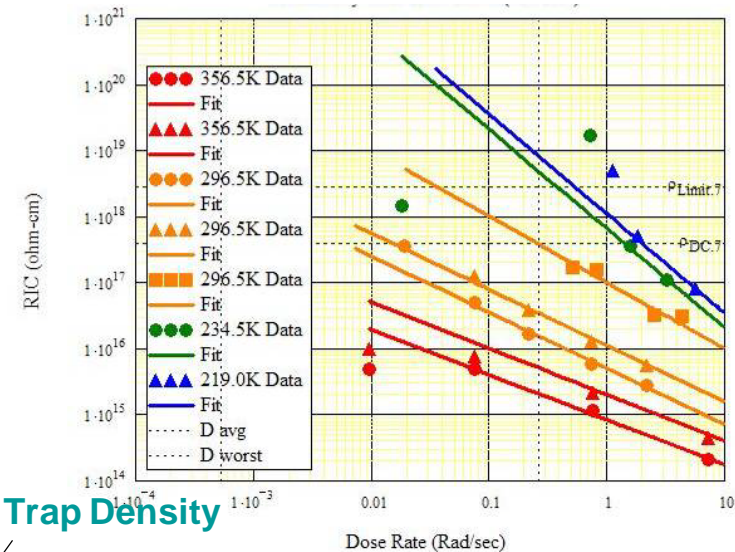
$$k(T) \rightarrow k_{RIC0}$$

Exponential Trap Density

$$\Delta(T) \rightarrow \frac{T_c}{T + T_c}$$

$$k(T) \rightarrow k_{RIC1} \left[2 \left(\frac{m_e k_B T}{2\pi \hbar^2} \right)^{3/2} \left(\frac{m_e^* m_h^*}{m_e m_e} \right)^{3/4} \right] \frac{T}{T + T_c}$$

$$\sigma_{RIC}(T, D) = k_{RIC}(T) \cdot D^{\Delta(T)}$$



Case V: Temperature and Dose Effects

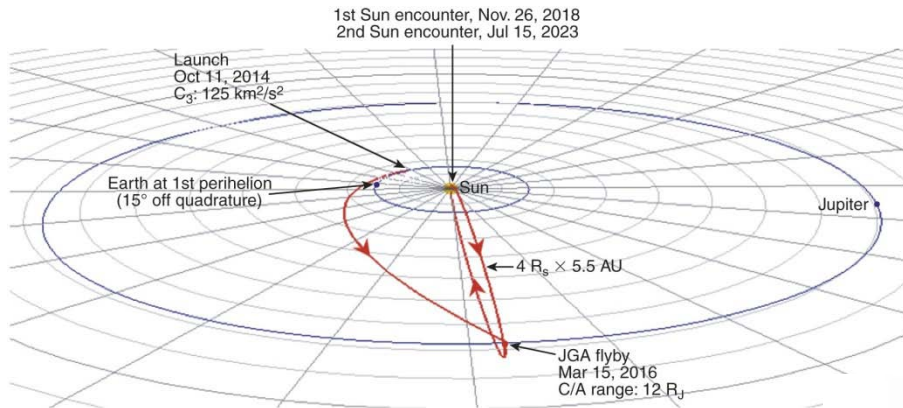


Figure 4-1. Solar Probe mission summary.

Wide Orbital Range
Earth to Jupiter Flyby
Solar Flyby to $4 R_S$

Wide Temperature Range
<100 K to >1800 K

Wide Dose Rate Range
Five orders of magnitude variation!

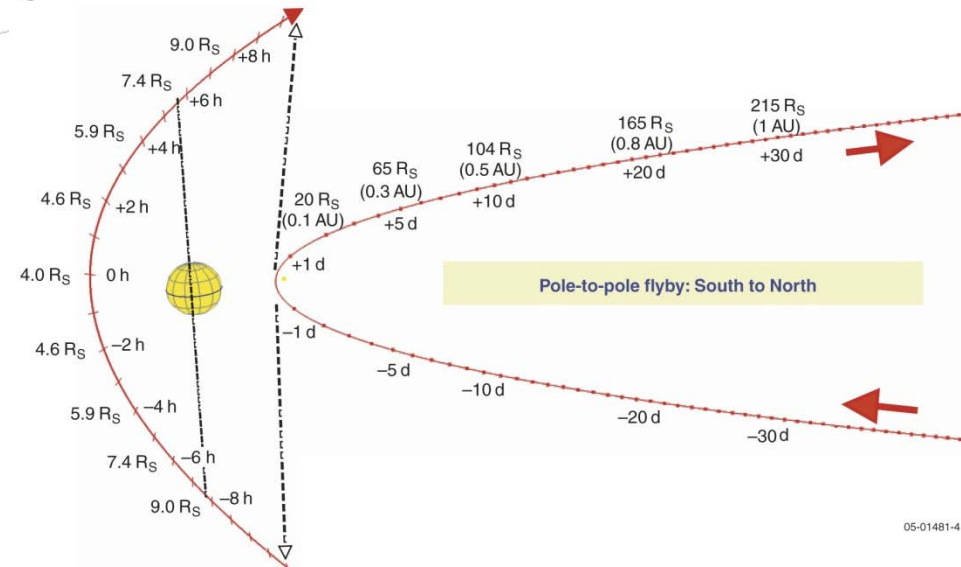


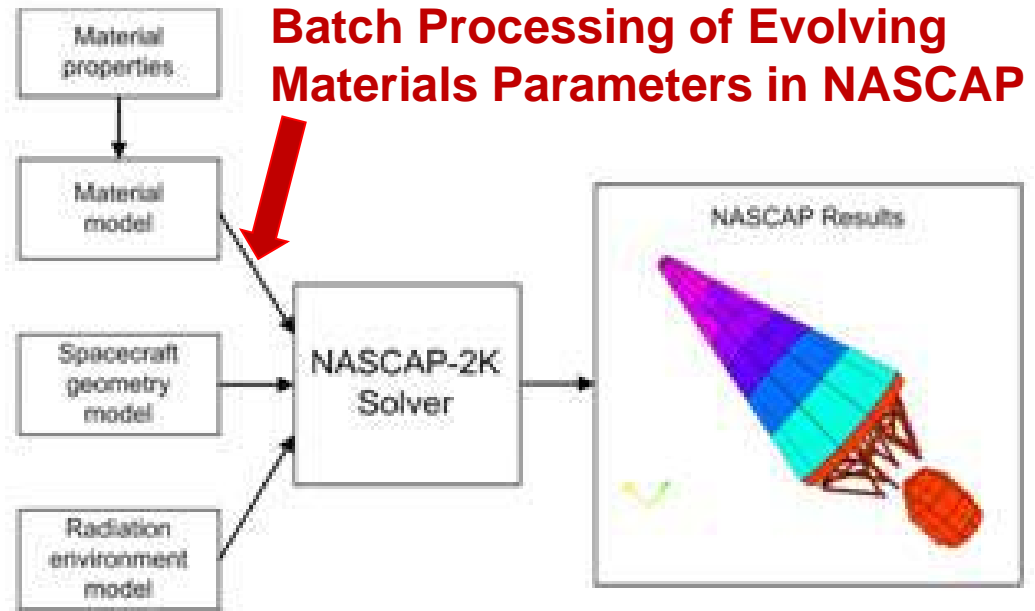
Figure 4-2. Solar encounter trajectory and timeline. Science operations begin at perihelion —5 days ($65 R_S$) and continue until perihelion +5 days.



Case V: Temperature and Dose Effects

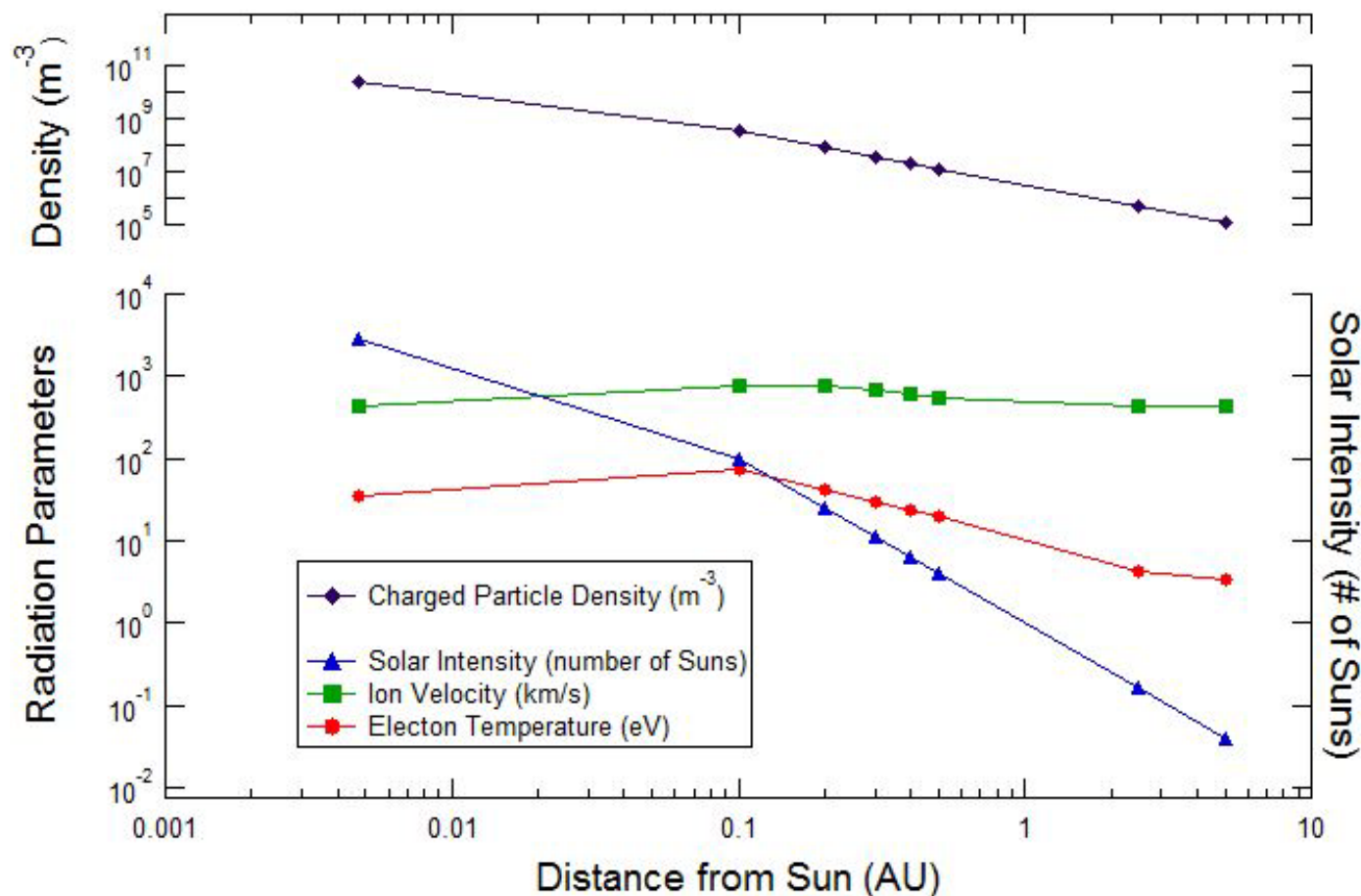
“We anticipate significant thermal and charging issues.”

J. Sample



- *Mission design by APL/GSFC*
- *Materials testing by Dennison and Hoffmann*
- *Evolutionary Charging Study by Donegan, Sample, Dennison & Hoffmann*
(See Donegann et al, JSR 2009)
- *Revised mission design and new charging study*
(See Donegann 11th SCTC Poster for update)

Case V: Temperature and Dose Effects



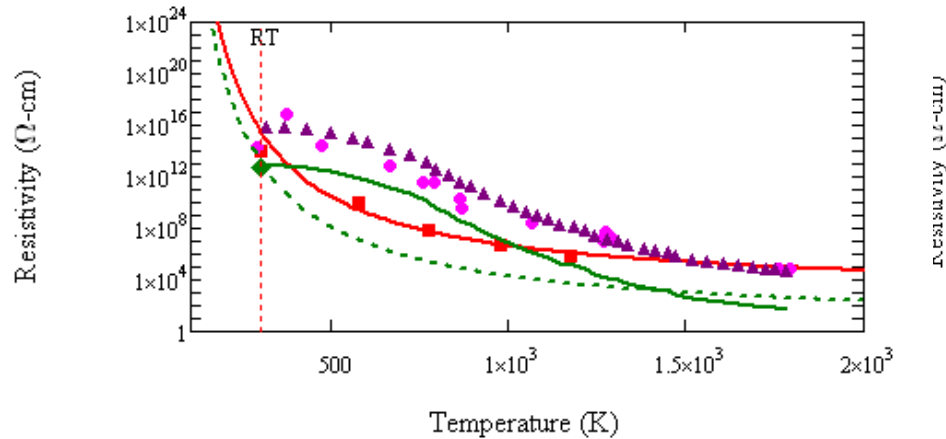
Wide Orbital Range
 Earth to Jupiter Flyby
 Solar Flyby to $4 R_s$

Wide Temperature Range
 $<100 \text{ K}$ to $>1800 \text{ K}$

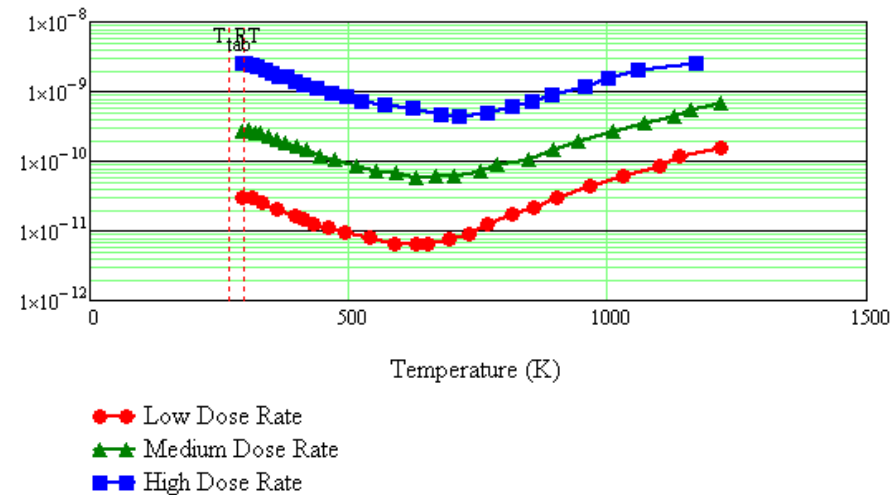
Wide Dose Rate Range
 Five orders of magnitude variation!

Case V: Temperature and Dose Effects

Dark Conductivity vs T



RIC vs T



Dark Conductivity

$$\sigma_{DC}(T) = \sigma_o^{DC} e^{-E_o/k_B T}$$

RIC

$$\sigma_{RIC}(T) = k_{RIC}(T) \dot{D}^{\Delta(T)}$$

Dielectric Constant

$$\epsilon_r(T) = \epsilon_{RT} + \Delta_\epsilon(T - 298 K)$$

Electrostatic Breakdown

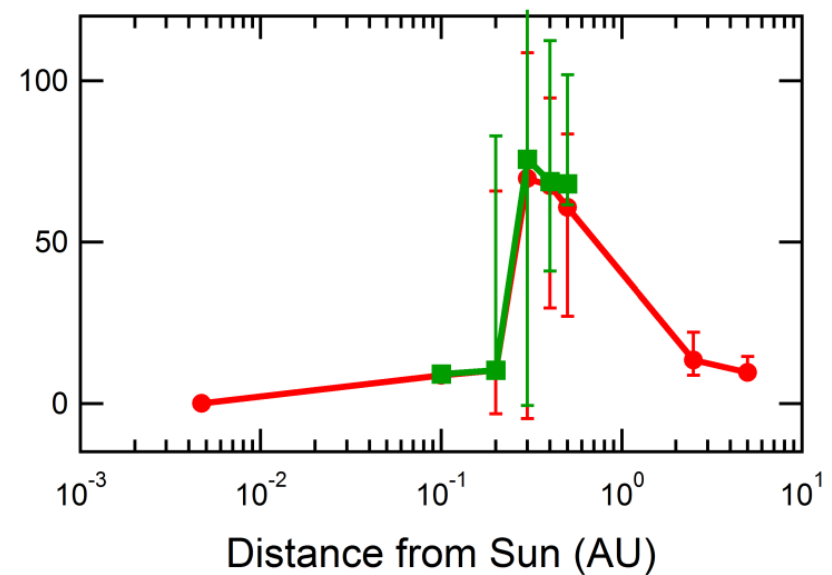
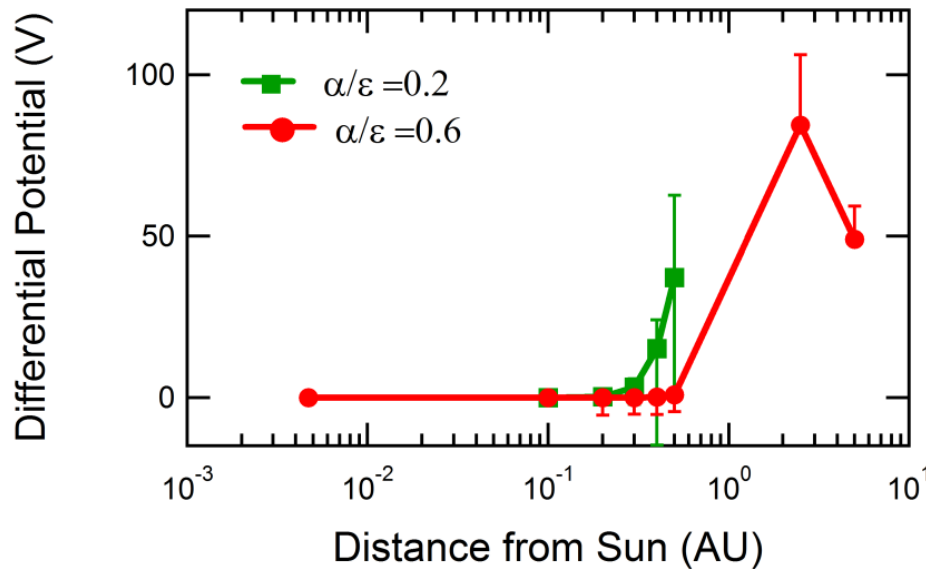
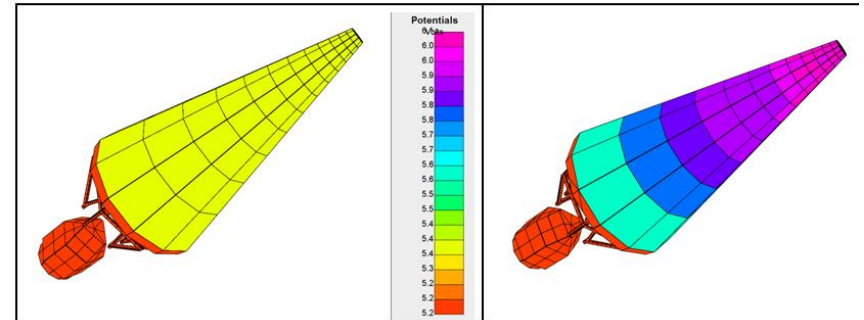
$$E_{ESD}(T) = E_{ESD}^{RT} e^{-\alpha_{ESD}(T - 298 K)}$$

Case V: Temperature and Dose Effects

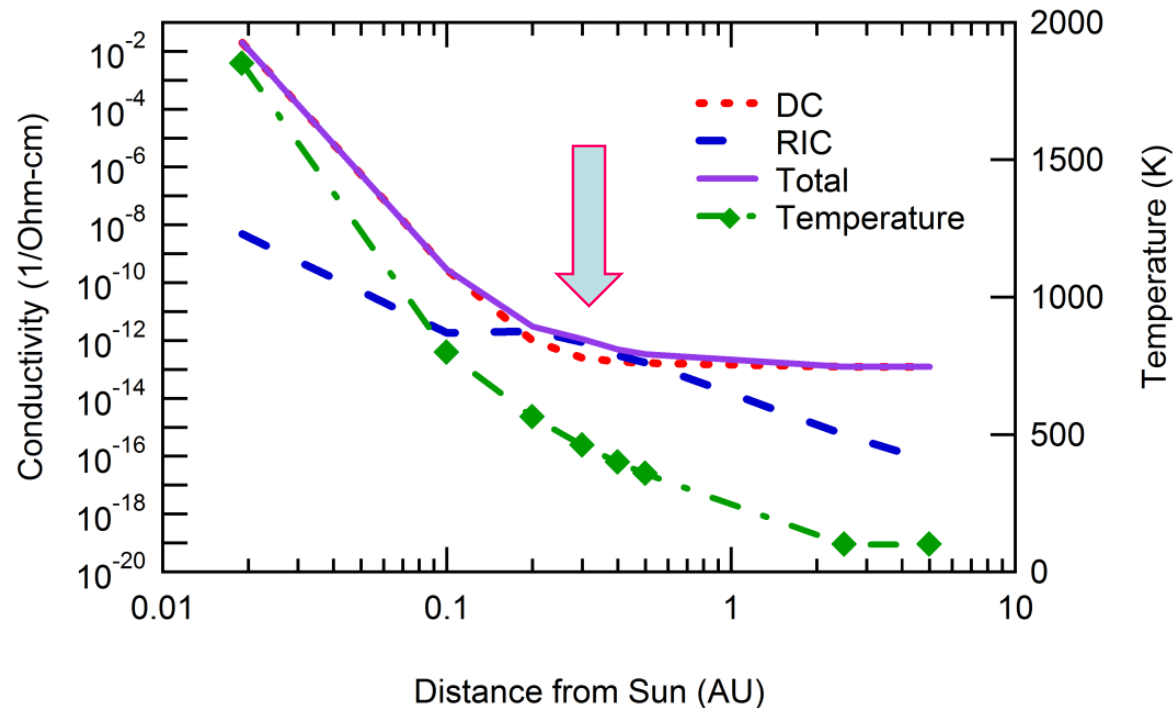
A peak in charging at
~0.3 to 2 AU

“...Curiouser and curiouser...”

--Alice



Case V: Temperature and Dose Effects



General Trends

Dose rate decreases as $\sim r^2$
 T decreases as $\sim e^{-r}$
 σ_{DC} decreases as $\sim e^{-1/T}$
 σ_{RIC} decreases as $\sim e^{-1/T}$
and decreases as $\sim r^2$

A fascinating trade-off

- *Charging increases from increased dose rate at closer orbits*
- *Charge dissipation from T -dependant conductivity increases faster at closer orbits*

Case VI: Multilayer/Nanocomposite Effects

Consider the Effects of Multilayer Materials, Composites, Contamination, or Oxidation

Length Scale

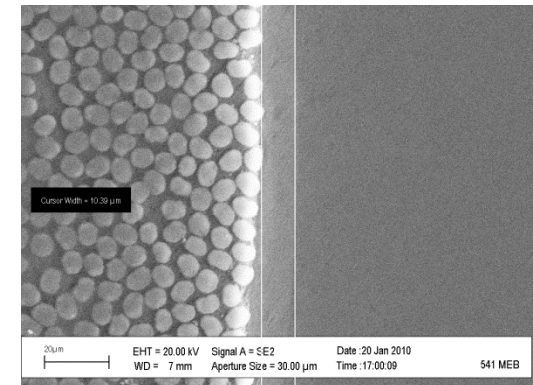
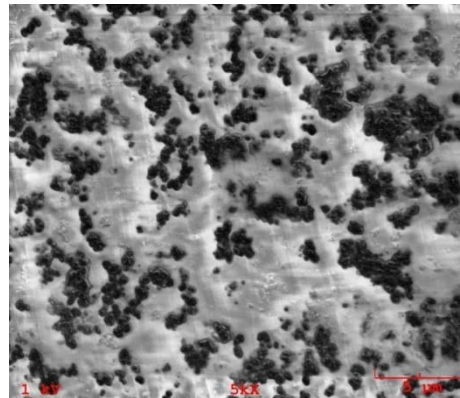
- Nanoscale structure of materials
- Electron penetration depth
- SE escape depth

Time Scales

- Deposition times
- Dissipation times
- Mission duration

Emission scaling depends on sample geometry and materials properties. May lead to:

- Power or flux scaling at different incident energies
- Energy or flux thresholds and/or cutoffs
- Significant emission from high energy e^-
- Significant emission from back sides or interior surfaces



10 μm

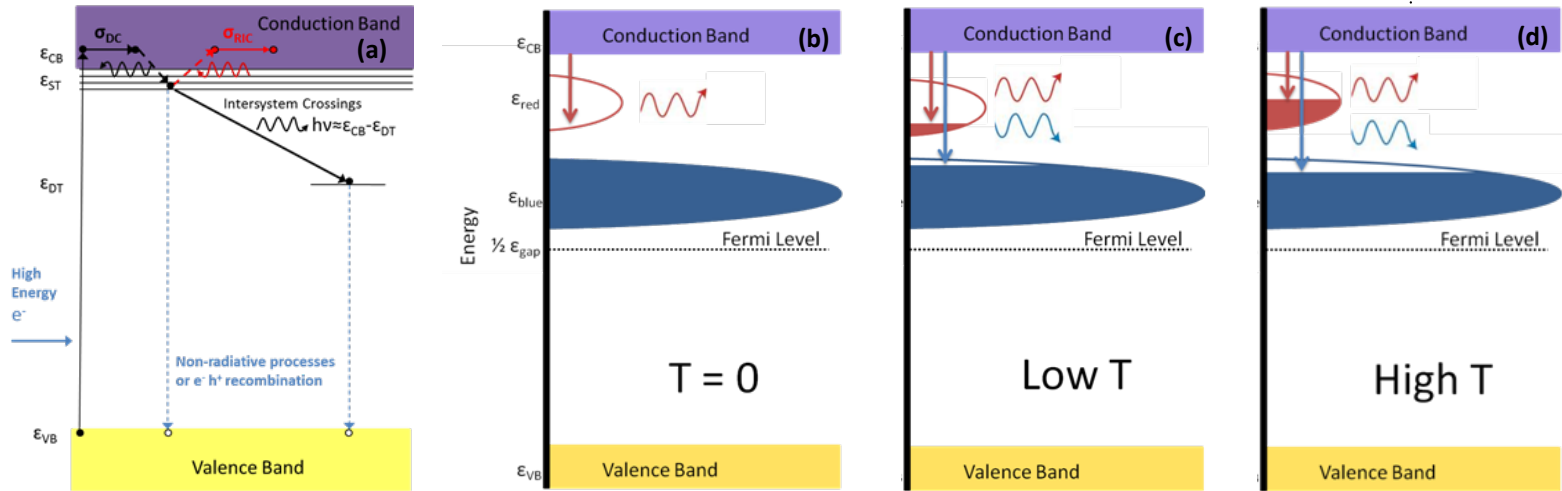


Fig. 2. Qualitative two-band model of occupied densities of state (DOS) as a function of temperature during cathodoluminescence. **(a)** Modified Joblonski diagram for electron-induced phosphorescence. Shown are the extended state valence (VB) and conduction (CB) bands, shallow trap (ST) states at ϵ_{ST} within $\sim k_B T$ below the CB edge, and two deep trap (DT) distributions centered at $\epsilon_{DT} = \epsilon_{red}$ and $\epsilon_{DT} = \epsilon_{blue}$. Energy depths are exaggerated for clarity. **(b)** At $T \approx 0$ K, the deeper DT band is filled, so that there is no blue photon emission if $\epsilon_{blue} < \epsilon_{eff}$. **(c)** At low T , electrons in deeper DT band are thermally excited to create a partially filled upper DT band (decreasing the available DOS for red photon emission) and a partially empty lower DT band (increasing the available DOS for blue photon emission). **(d)** At higher T , enhanced thermal excitations further decrease red photon emission and increase blue photon emission. Radiation induced

$$I_Y(J_b, E_b, T, \lambda) \propto \dot{D}(J_b, E_b) \left[\frac{1}{\dot{D} + \dot{D}_{sat}} \left(\frac{\epsilon_{ST}}{k_B T} \right) \right] \{ A_f(\lambda) [1 + \mathbb{R}_m(\lambda)] \} \quad (1)$$

where dose rate \dot{D} (absorbed power per unit mass) is given by

$$\dot{D}(J_b, E_b) = \frac{E_b J_b [1 - \eta(E_b)]}{q_e \rho_m} \times \begin{cases} [1/L] & ; R(E_b) < L \\ [1/R(E_b)] & ; R(E_b) > L \end{cases} \quad (2)$$

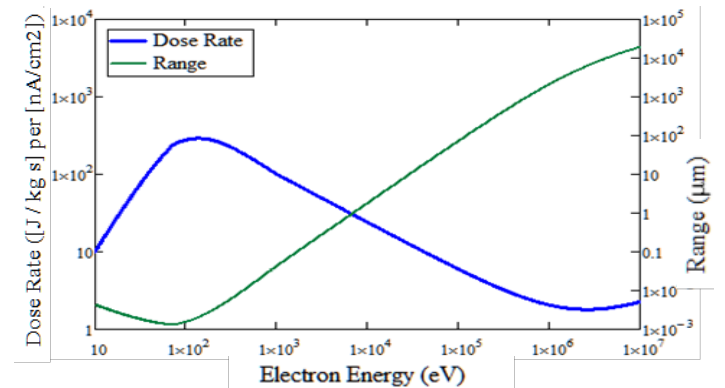


Fig. 3. Range and dose rate of disordered SiO₂ as a function of incident energy using calculation methods and the continuous slow-down approximation described in [5].

Measured Cathodolumuminescence Intensity in Fused Silica

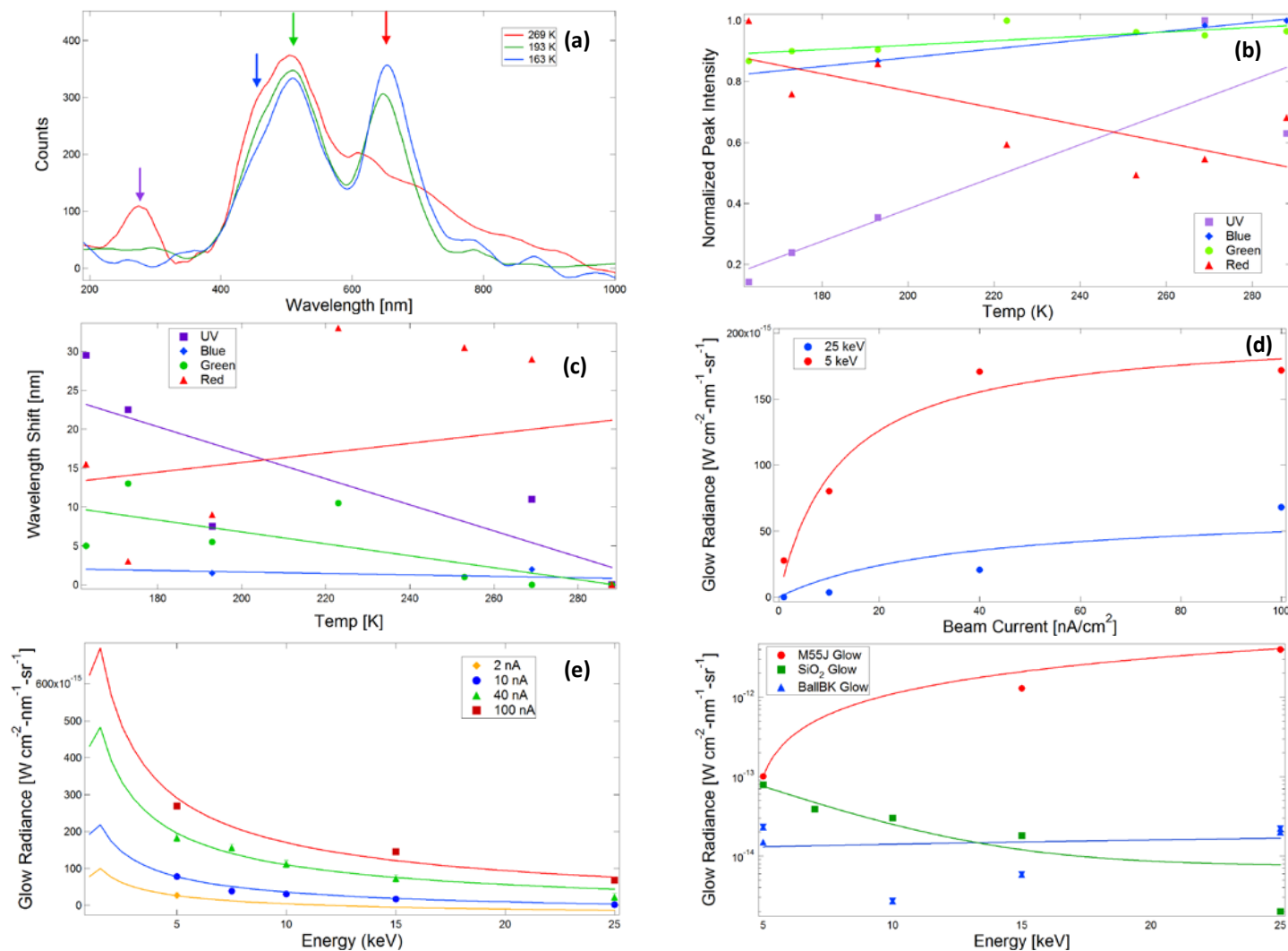
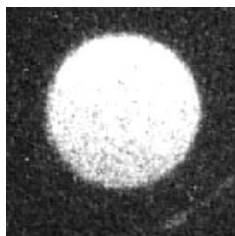


Fig. 1. Optical measurements of luminescent thin film disordered SiO₂ samples. **(a)** Three luminescence UV/VIS spectra at decreasing sample temperature. Four peaks are identified: red (~645 nm), green (~500 nm), blue (~455 nm) and UV (275 nm). **(b)** Peak amplitudes as a function of sample temperature, with baseline subtracted and normalized to maximum amplitudes. **(c)** Peak wavelength shift as a function of sample temperature. **(d)** Total luminescent radiance versus beam current at fixed incident energy fit by (1). **(e)** Total luminescent radiance versus beam energy at fixed incident flux fit by (1). **(f)** Total luminescent radiance versus beam energy at fixed 10 nA/cm² incident flux for epoxy-resin M55J carbon composite (red; linear fit), SiO₂ coated mirror (green; fit with (1)), and

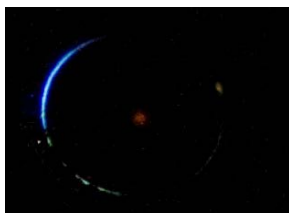
Diversity of Emission Phenomena in Black Kapton

Ball Black Kapton	22 keV	110 or 4100 $\mu\text{W}/\text{cm}^2$
Runs 131 and 131A	135 K	5 or 188 nA/cm^2



Surface Glow

Relatively low intensity
Always present over full surface when e-beam on
May decay slowly with time



Edge Glow

Similar to Surface Glow,
but present only at sample edge



1



2



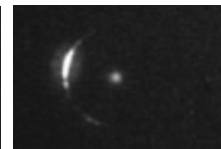
1



2



3



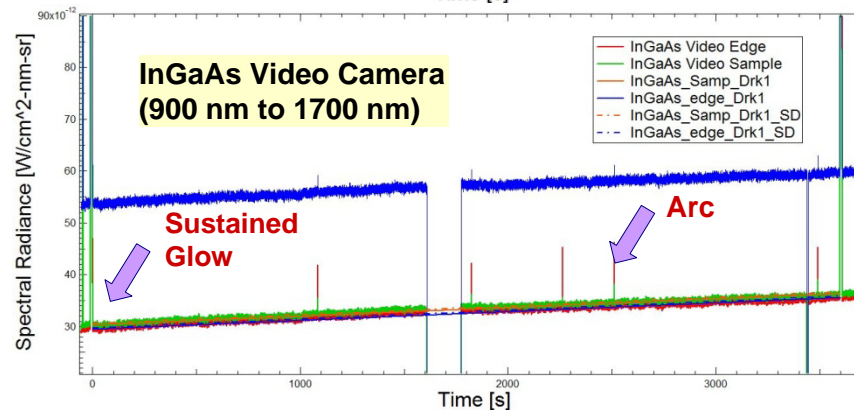
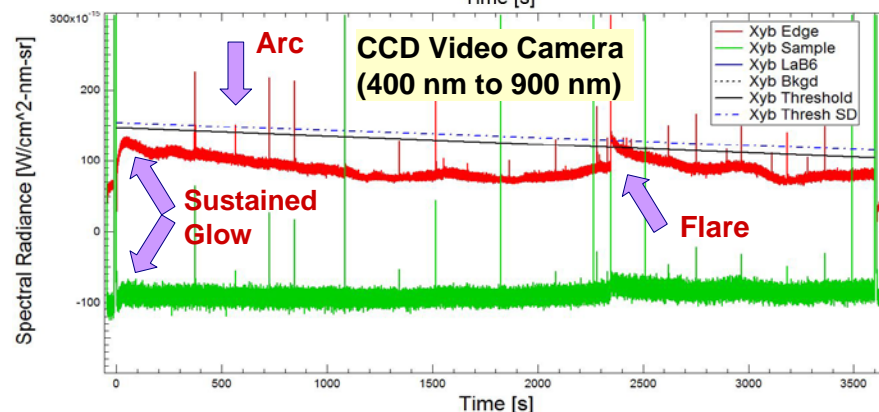
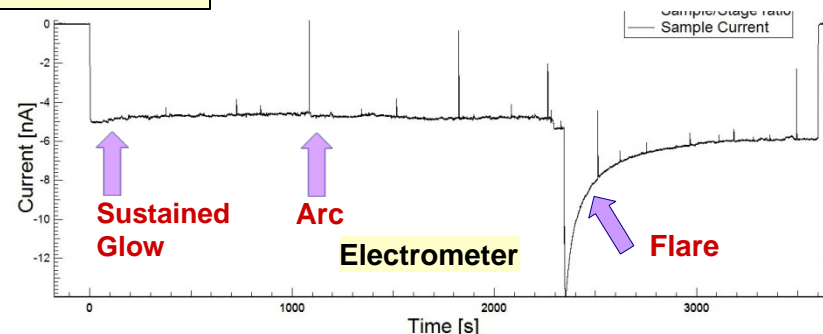
4

"Flare"

2-20x glow intensity
Abrupt onset
2-10 min decay time

Arc

Relatively very high intensity
10-1000X glow intensity
Very rapid <1 μs to 1 s

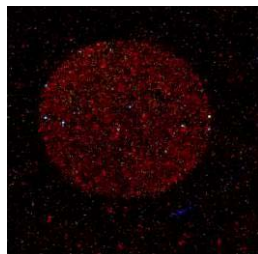


Comparison of Luminescence Images

Sustained Glow

Kapton XC

500 nA/cm²
22 keV
150 K



M55J

1 nA/cm²
22 keV
100 K



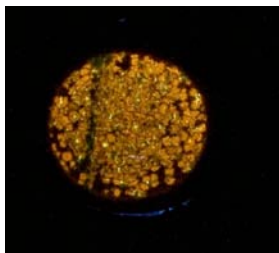
IEC Shell Face
Epoxy Resin with
Carbon Veil

1 nA/cm²
22 keV
100 K



Kapton E

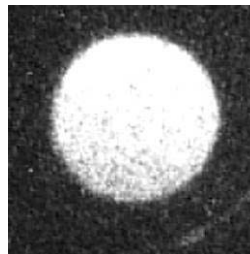
500 nA/cm²
22 keV
150 K



"Flare"

Kapton XC

50 nA/cm²
22 keV
150 K



M55J

1 nA/cm²
22 keV
100 K



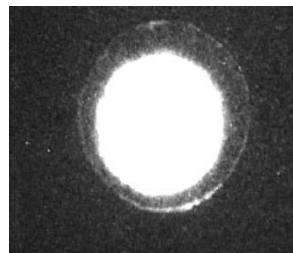
IEC Shell Face
Epoxy Resin
with Carbon Veil

1 nA/cm²
22 keV
100 K



Kapton E

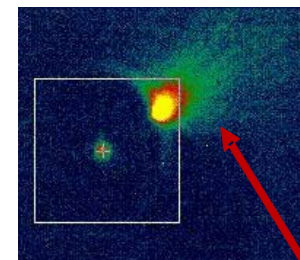
5 uA/cm²
22 keV
150 K



Arcs

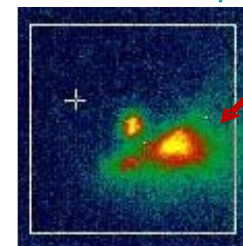
Kapton XC

5 nA/cm²
22 keV
1350 K



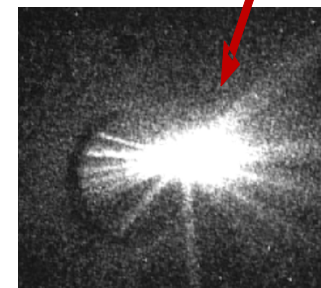
M55J

5 nA/cm²
22 keV
135 K



IEC Shell Face
Epoxy Resin
with Carbon Veil

5 nA/cm²
22 keV
100 K



1 cm Dia test samples

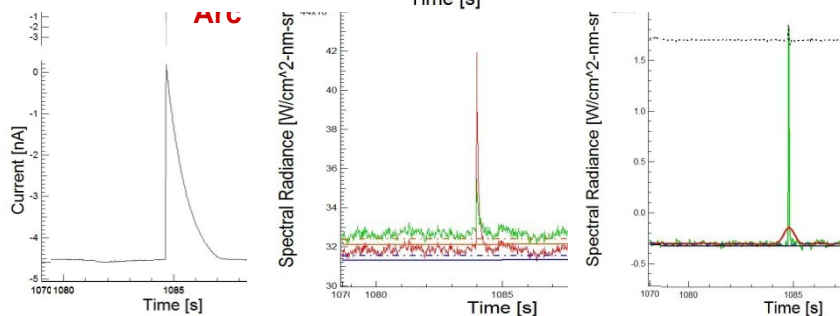
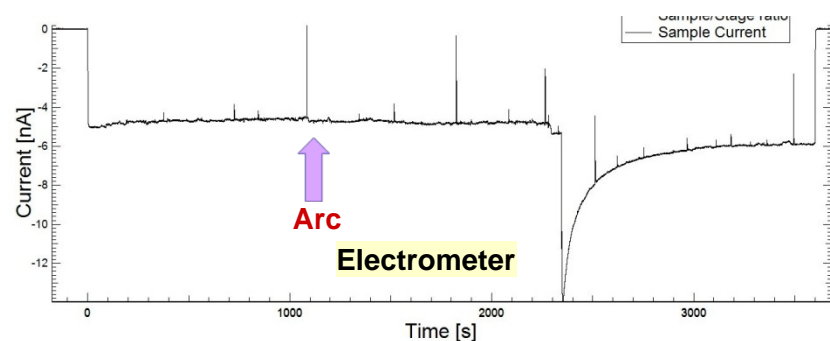
30 s Exposure SLR Camera
(400nm-640nm)

33 ms Exposure CCD Video Camera
(500nm-900nm)

17 ms Exposure InGaAs Video Camera
(900nm-1700nm)

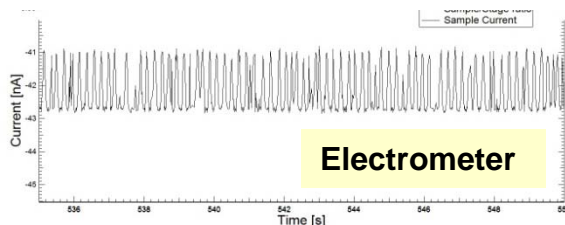
Arcs Observed in Black Kapton and M55J

Ball Black Kapton 22 keV 110 or 4100 $\mu\text{W}/\text{cm}^2$
Runs 131 and 131A 135 K 5 or 188 nA/cm^2



Electrometer InGaAs Video CCD Video

Rapid Arcing at
4 mW/cm^2
~20000 arcs/hr

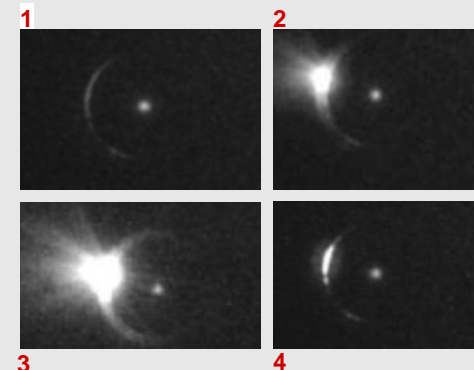


Arc Characteristics

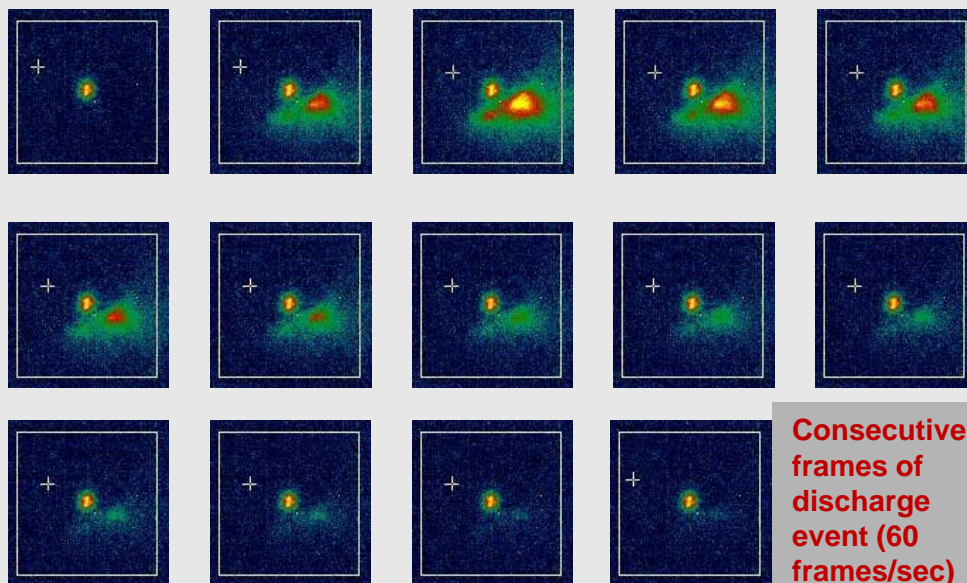
Arc duration:
~0.2 to 0.8 s in electrometers
and video cameras

Arc Freq. at 110 $\mu\text{W}/\text{cm}^2$:
~10 arcs/hr for Black Kapton
~30 arcs/hr for M55J

Arc Intensity:
~ 10X to 1000X glow amplitude
~5% to 20% of glow power



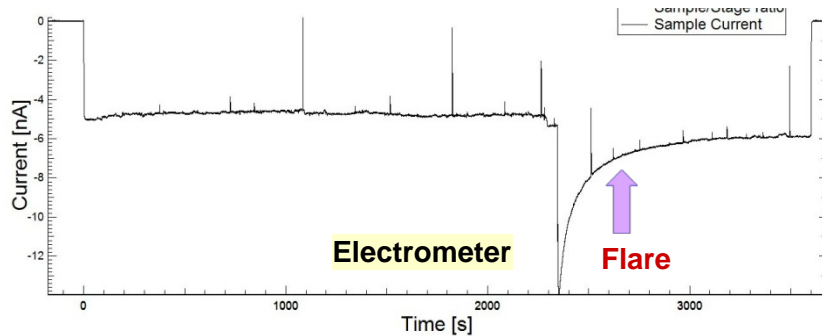
CCD camera (400nm-900nm)



Consecutive
frames of
discharge
event (60
frames/sec)

InGaAs camera (900nm-1700nm)

“Flares” Observed in Black Kapton



Ball Black Kapton

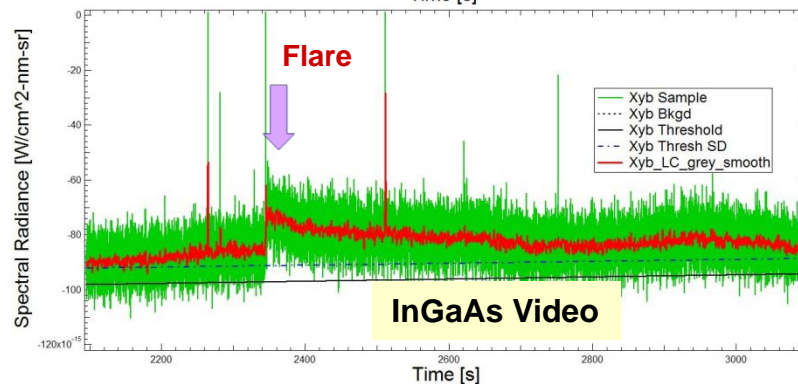
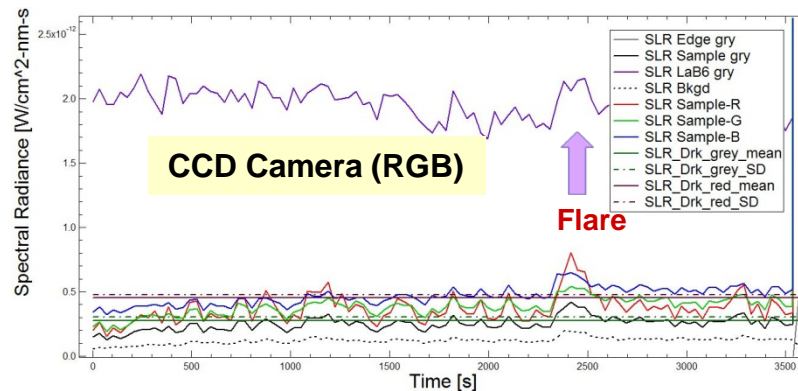
Runs 131

110 $\mu\text{W}/\text{cm}^2$

5 nA/cm^2

22 keV

135 K



“Flare” Characteristics

“Flare” duration:

Abrupt onset

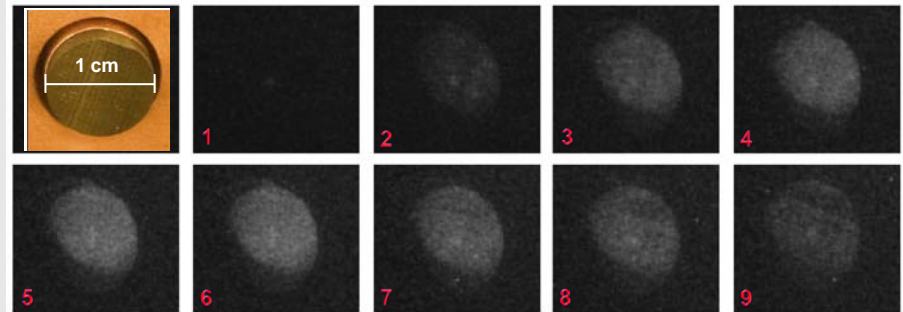
~2-10 min exp. decay time
in electrometers and video
cameras

“Flare” Frequency:

0-2 flares/hr

“Flare” Intensity:

~ 2X to 20X glow amplitude
~5% to 20% of glow power



CCD camera
(400nm-900nm)

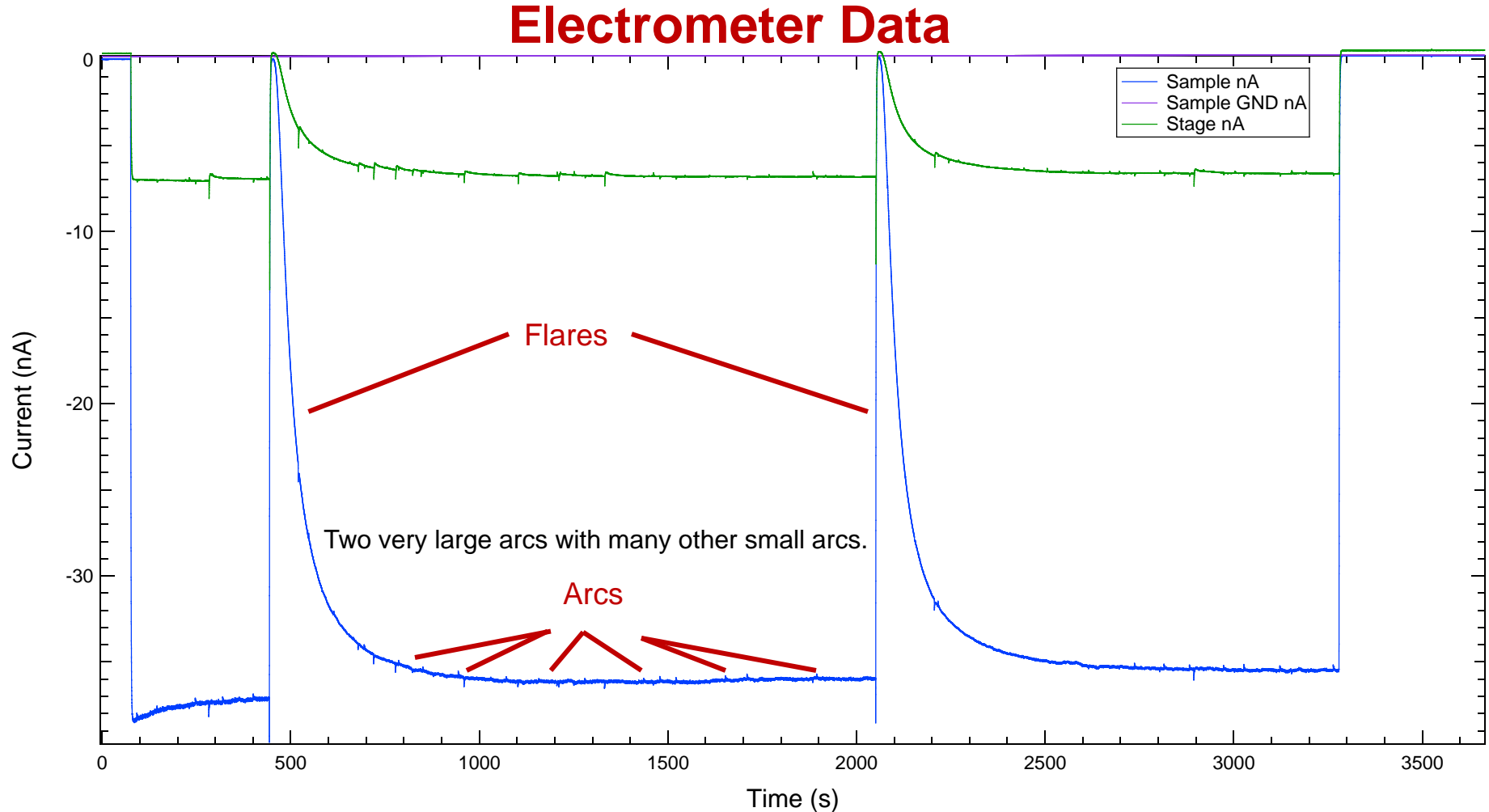
M55J

5 nA/cm^2

22 keV

135 K

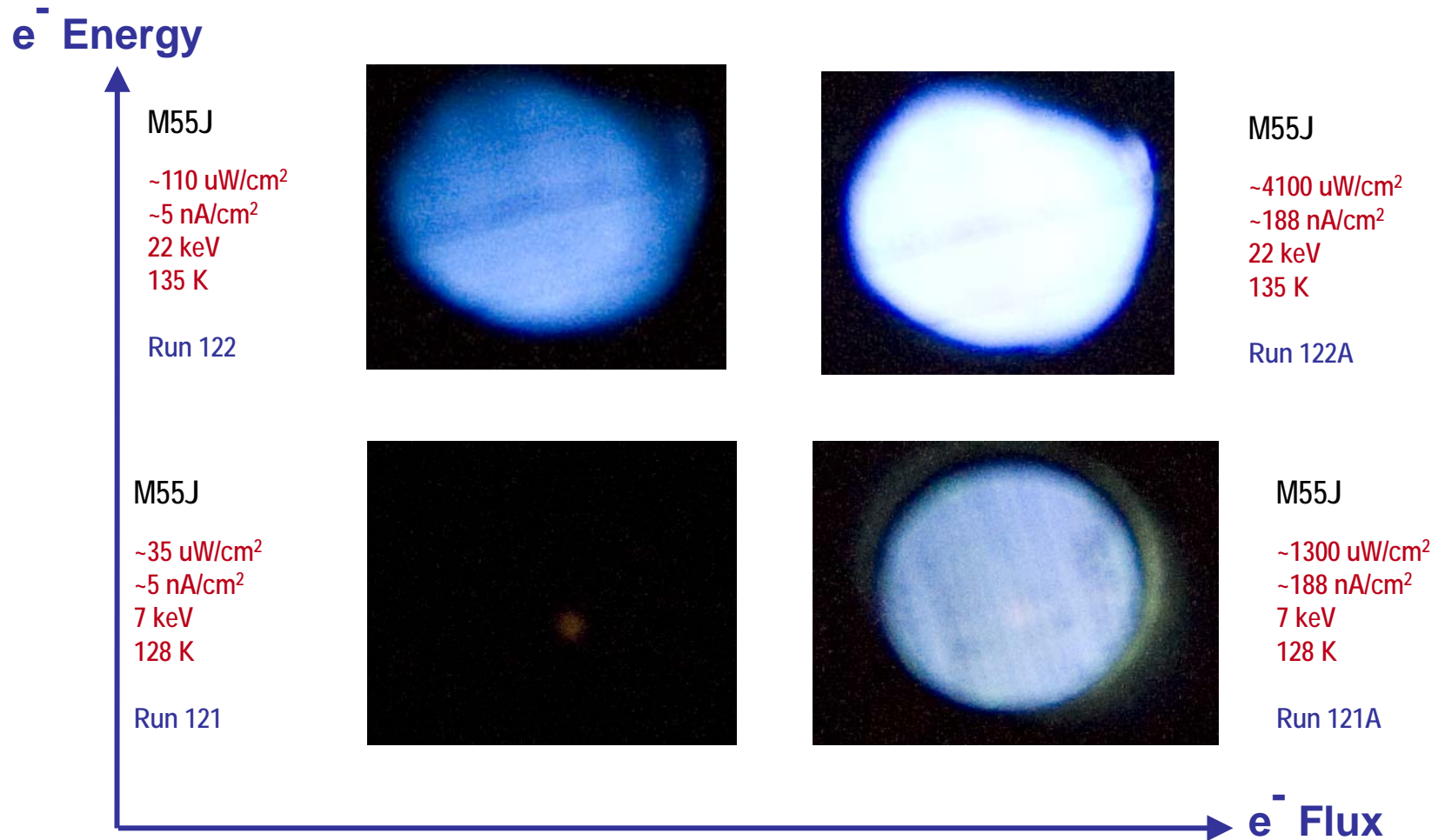
Details of Electrometer “Flare” Signature



Total Beam Time: 3204 s
of Arcs: >50

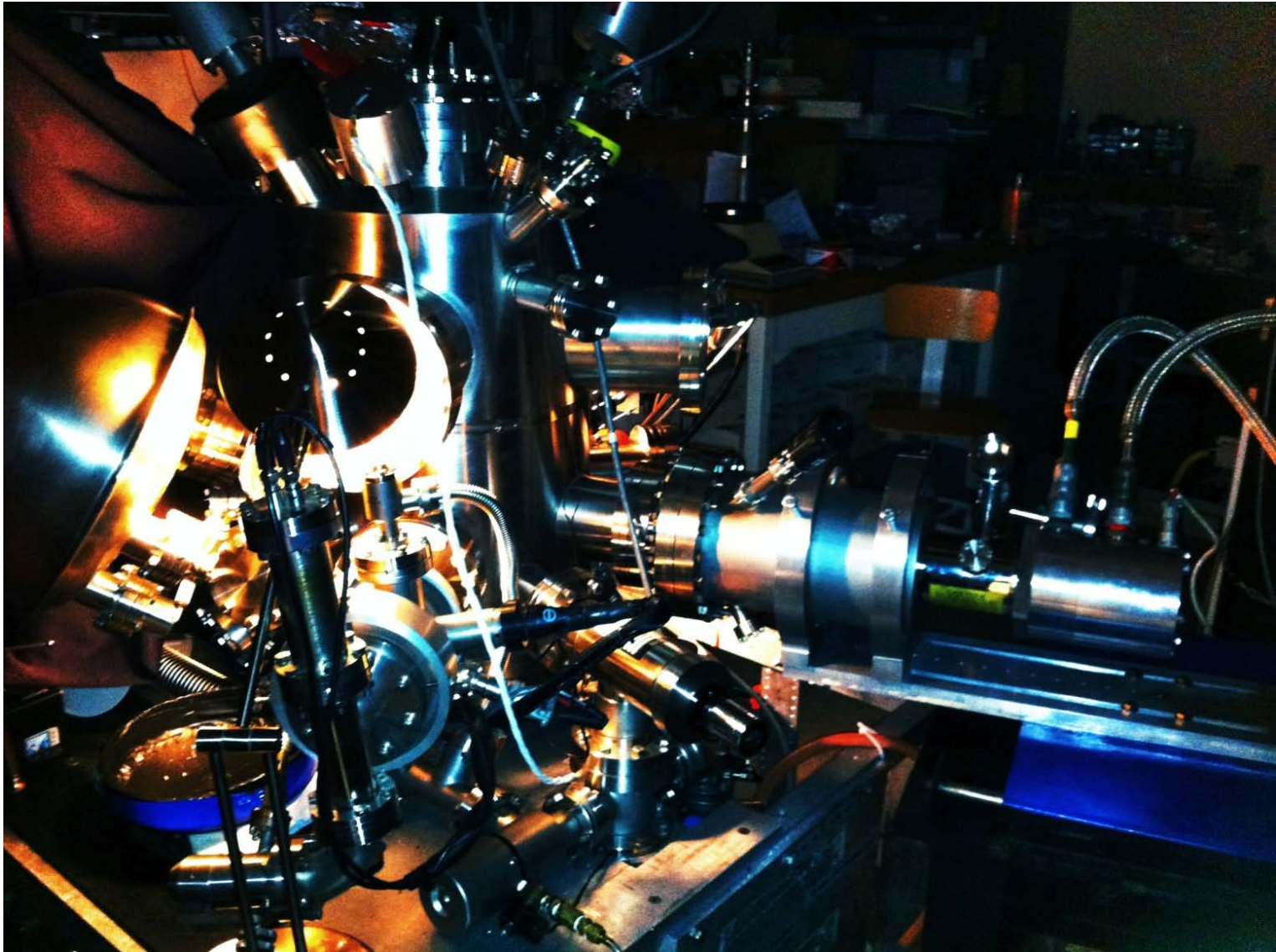
**High Conductivity
C-loaded Kapton
25keV 38nA ~1 hr**

Glow Increases with Increasing Flux, Energy and Power



- Surface Glow, Edge Glow, and Arcing Frequency are all found to increase with increasing incident electron flux and energy.
- Insufficient data for trends to establish functional dependence and possible thresholds or cut-offs

End with a Bang



Supplemental Slides

Theoretical modeling of the interplay between electron-induced luminescence and radiation induced conductivity in highly disordered insulating materials.

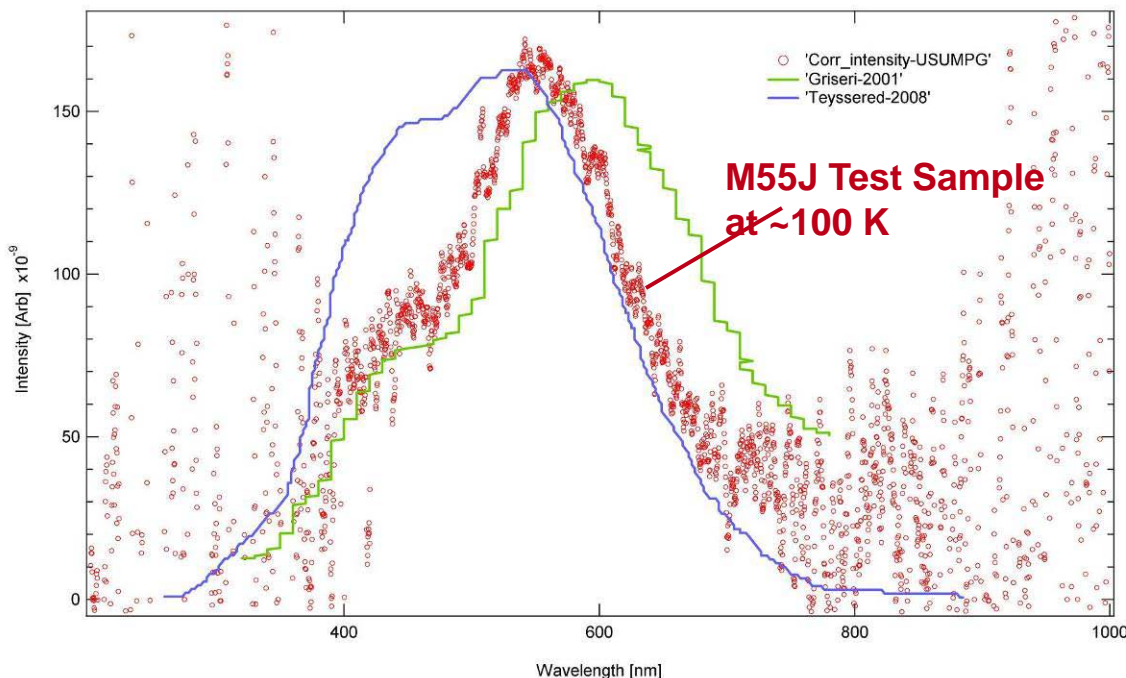
Grisseri, Teyssedre and others have done groundbreaking work on electron induced luminescence that Jensen and Dennison at USU have extended to lower temperatures.

Merging our work should lead to interesting results.

Absolute Photon Yield per Incident Electron

Current Best Estimate of Photon Invariant Factor for M55J Glow at L2 “High Storm” Incident Electron Flux at Cryogenic Temperatures

$7 \cdot 10^7$ photon/cm²-s-sr-nm



Electron-Induced Luminescence Spectra

=====

±200% based of average of 4 independent calibration methods and uncertainties in optics losses, spectral profiles, sample geometries and experimental methods

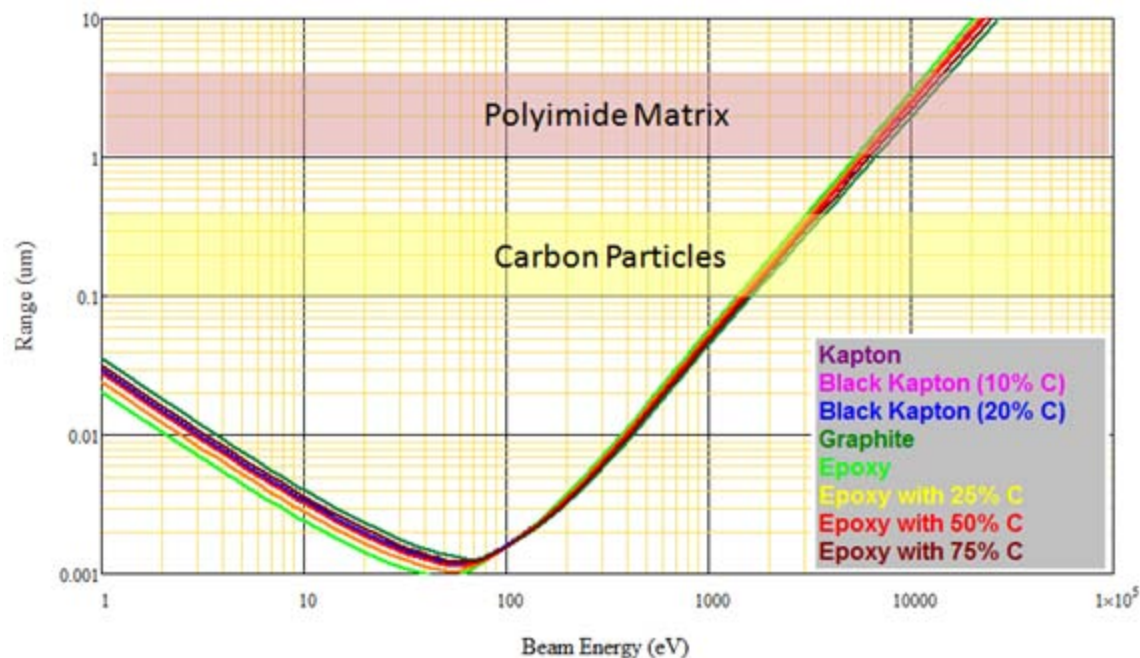
- Observed first at USU
- Glow visible on Kapton XC, Kapton E and M55J, T300 and Fiberglass composite materials
- Tests qualitatively confirmed at MSFC and Northrop-Grumman
- Consistent with RT test of similar materials in literature by ONERA and limited available physics models

- Overlap of work that Griseri and Dennison are both currently engaged in, related to use of the pulsed electroacoustic (PEA/PWP) method for probing embedded charge layers.

USU had our first successful PEA measurement of charge layer dynamics last night.

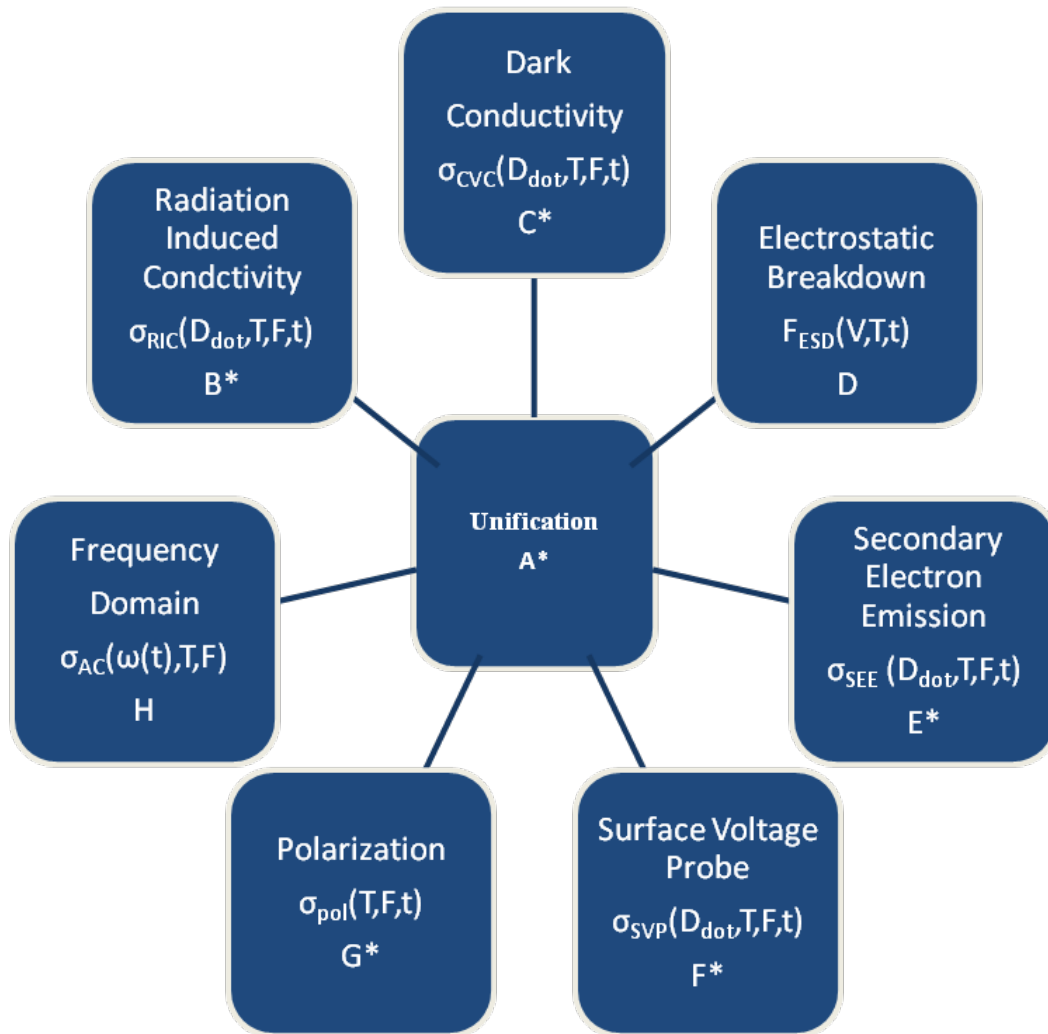
The lesson is that it pays to leave the lab and go enjoy fine French cuisine!

- Comparison of codes to model electron penetration and charge deposition in insulators. This has important overlaps with the PEA work listed above.



Review of work on generalized density of states models for localized trap states in highly disordered materials developed at USU, and their applications to theoretical models being worked on in Toulouse.

Just a drop in the bucket...



Complete set of dynamic transport equations

$$J = q_e n_e(z, t) \mu_e F(z, t) + q_e D \frac{dn_{tot}(z, t)}{dz}$$

$$\frac{\partial}{\partial z} F(z, t) = q_e n_{tot} / \epsilon_0 \epsilon_r$$

$$\frac{\partial n_{tot}(z, t)}{\partial t} - \mu_e \frac{\partial}{\partial z} [n_e(z, t) F(z, t)] - q_e D \frac{\partial^2 n_e(z, t)}{\partial z^2} = N_{ex} -$$

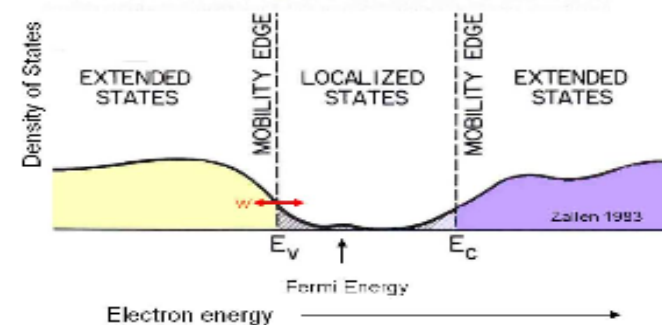
$$\alpha_{er} n_e(z, t) n_{tot}(z, t) + \alpha_{et} n_e(t) [N_t(z) - n_t(z, t)]$$

$$\frac{dn_h(z, t)}{dt} = N_{ex} - \alpha_{er} n_e(z, t) n_h(z, t)$$

$$\frac{dn_t(z, \epsilon, t)}{dt} = \alpha_{et} n_e(z, t) [N_t(z, \epsilon) - n_t(z, \epsilon, t)] -$$

$$\alpha_{te} N_e \exp\left[-\frac{\epsilon}{kT}\right] n_t(z, \epsilon, t)$$

A quantum mechanical model of the spatial and energy distribution of the electron states



Overlaps of work with secondary electron emission with Mohamed Belhaj. Specifically, it would be interesting to work in collaboration with the PhD student you mentioned (from Université Paul Sabatier, I believe) who is studying secondary electron emission measurements/effects of bulk charging. This work dovetails nicely with studies done on the subject at USU by Dennison, Wilson, Hoffmann and Hodges.

Low Charge Capabilities

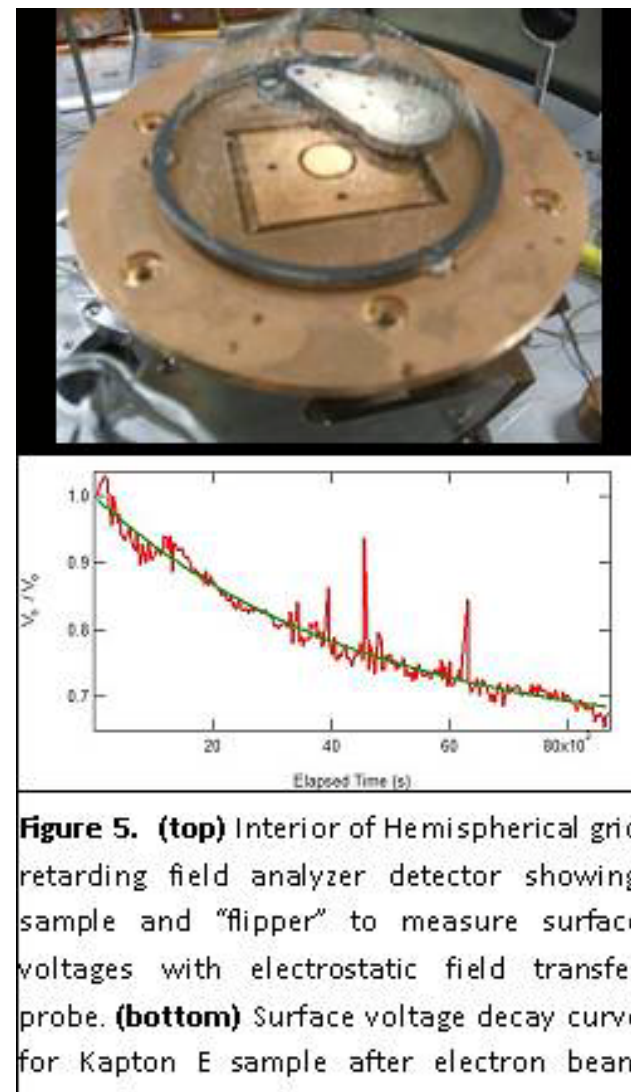
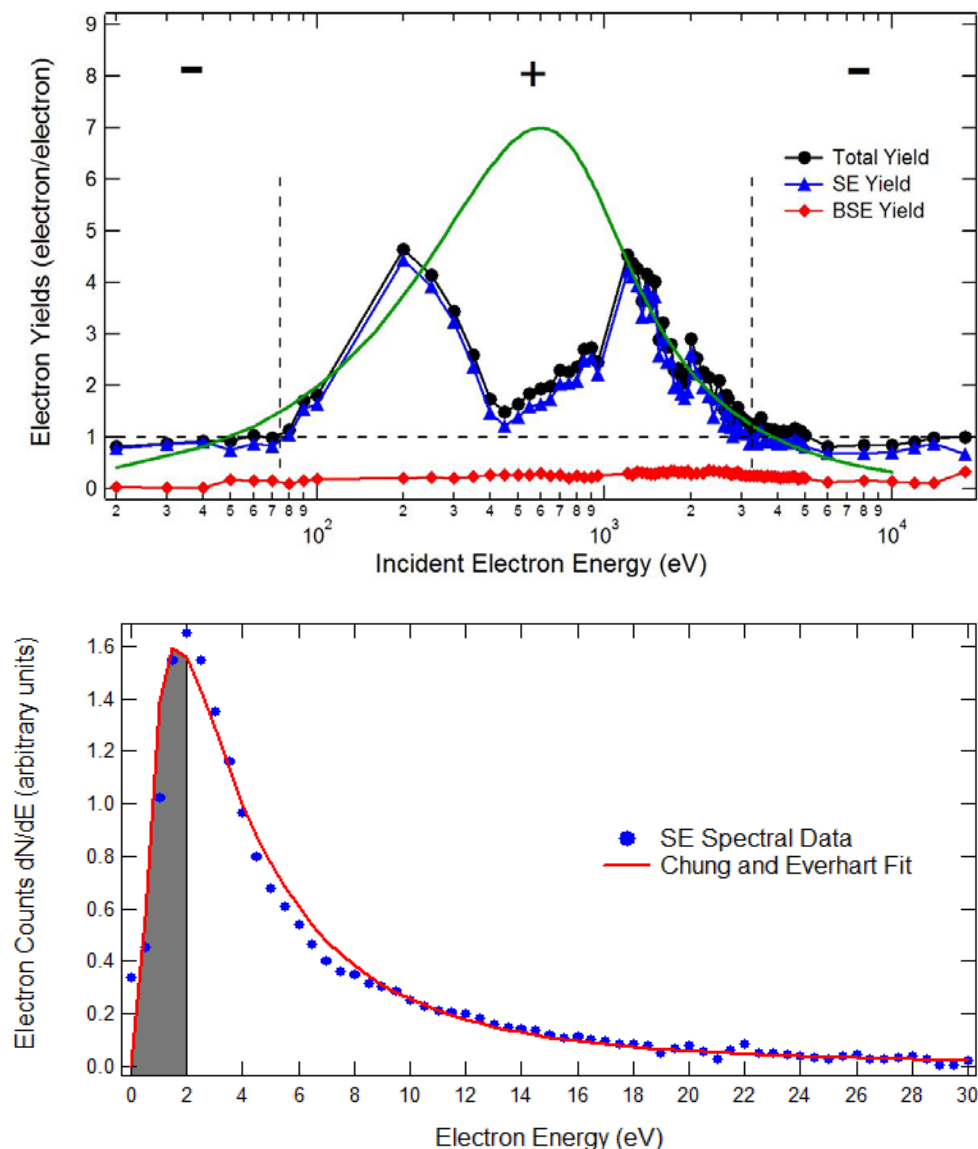
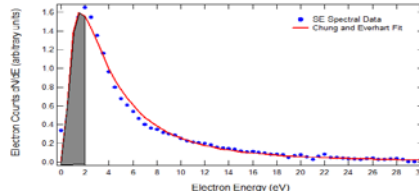


Figure 5. (top) Interior of Hemispherical grid retarding field analyzer detector showing sample and "flipper" to measure surface voltages with electrostatic field transfer probe. **(bottom)** Surface voltage decay curve for Kapton E sample after electron beam

Combining all the pieces

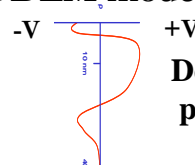
$$\frac{\delta_i(E_o, Q_i)}{\delta_o(E_o)} = \frac{\int_{0 \text{ eV}}^{50 \text{ eV}} \frac{dN(E; E_o)}{dE} dE}{\int_{0 \text{ eV}}^{50 \text{ eV}} \frac{dN(E; E_o)}{dE} dE} \leftarrow eV_s(Q_i)$$

Physics based model for yield SE recapture as a function of incident fluence



$$V_s = \frac{Q_o(\sigma - 1)d}{\epsilon_o \epsilon_r A_o} - \frac{\sigma Q_o \lambda_{SE} + Q_o R}{2 \epsilon_o \epsilon_r A_o}$$

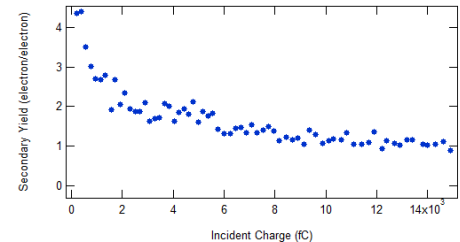
DDL model for surface potential



Depth profile for net positive charging

$$\sigma(E_o Q) = \eta(E_o) + \delta(E_o Q)$$

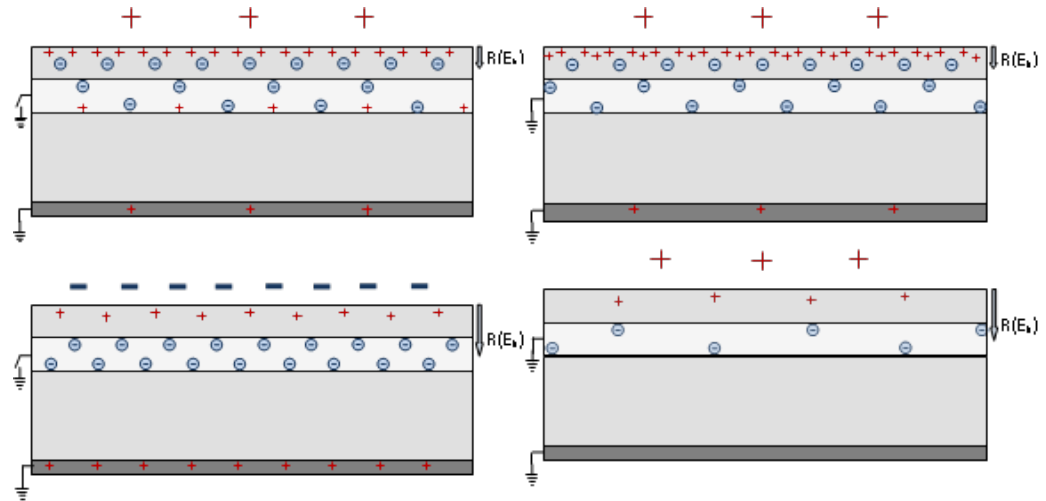
Decay curve data



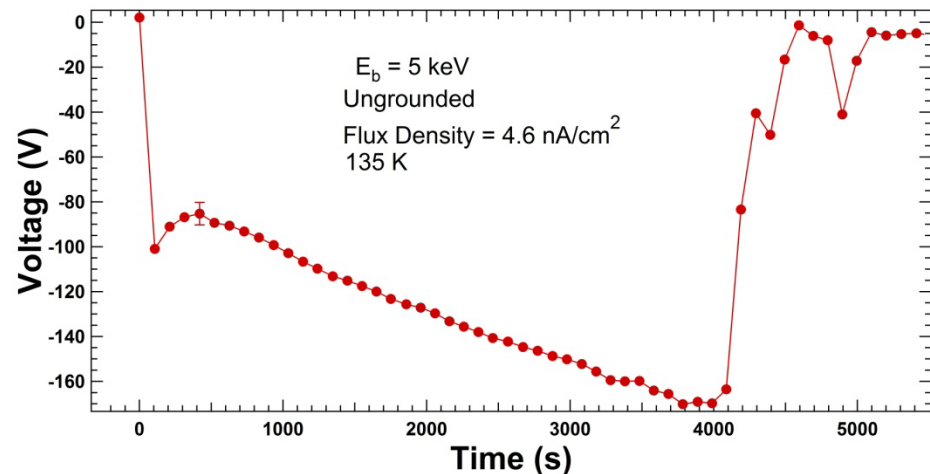
$$\delta(eV_s) = (\sigma_o(E_o) - 1) \cdot \left(1 - \frac{\lambda_{se}}{2 \cdot d}\right) \cdot \left(\frac{\frac{h(\epsilon_s)}{h(50 \cdot eV)} - 1}{\frac{h(0)}{h(50 \cdot eV)} - 1} \right) - \left[\eta_o \cdot \left(1 - \frac{\lambda_{se}}{2 \cdot d}\right) - \left(1 + \frac{R}{2 \cdot d}\right) \right]$$

We now have an analytic solution for secondary electron yield as surface potential changes in response to incident charge.

Surface conductivity of insulating materials as measured with surface potential probes and conductivity measurements. These include both lateral currents and charge transport with the RIC region.



Both the French group and USU have observed similar interesting anomalous behavior in materials. Thierry Paulmier, Phillipe. Molinié, Rachel Hanna and others have developed theoretical explanations for these anomalous phenomena that we hope to reconcile with our theoretical/empirical understanding. Both groups have taken complementary



Comparison of numerical fitting models for secondary and backscattered electron emission, photoemission, ion-induced emission, radiation induced conductivity and conductivity used in the US and ESA spacecraft charging codes.

The ISO (International Standards Organization) Workshop in Tokyo began the process of establishing an international standard for Extreme Space Environments for Spacecraft Charging Applications. This is an ongoing effort of critical importance to the spacecraft industry. Initial efforts were also begun at this meeting to organize a round robin testing of spacecraft materials properties used for simulations of spacecraft charging. USU and LAPACE/ONERA are two of the lead institutions in this effort. I propose to work with the French group to further this effort and identify concrete objectives and tests to get this going.

